THE INVESTIGATION OF BIODEGRADABLE CORROSION PROPERTIES OF HOT ROLLED AT31 MG ALLOYS

2022
MASTER THESIS
METALLURGICAL AND MATERIALS ENGINEERING

Ahmed Saad NAJM AL-GBURI

Thesis Advisor
Assist. Prof. Dr. Ismail Hakkı KARA

THE INVESTIGATION OF BIODEGRADABLE CORROSION PROPERTIES OF HOT ROLLED AT31 MG ALLOYS

Ahmed Saad NAJM AL-GBURI

T.C.
Karabuk University
Institute of Graduate Programs
Department of Metallurgical and Materials Engineering
Prepared as
Master Thesis

Thesis Advisor
Assist. Prof. Dr. Ismail Hakkı KARA

KARABUK
June 2022

I certify that in my opinion the thesis submitted by Ahmed Saad titled “THE INVESTIGATION OF BIODEGRADABLE CORROSION PROPERTIES OF HOT ROLLED AT31 MG ALLOYS” is fully adequate in scope and in quality as a thesis for the degree of Master of Science.

Assist. Prof. Dr. İsmail Hakkı KARA .....
Thesis Advisor, Department of Metallurgical And Materials Engineering

This thesis is accepted by the examining committee with a unanimous vote in the Department of Metallurgical and Materials Engineering as a Master of Science thesis. Jun 20, 2022

Examining Committee Members (Institutions)	Signature
Chairman : Prof. Dr. Mustafa ACARER (SU)	.....
Member : Prof. Dr. Hayrettin AHLATCI (KBU)	.....
Member : Assist. Prof. Dr. İsmail Hakkı KARA (KBU)	.....

The degree of Master of Science by the thesis submitted is approved by the Administrative Board of the Institute of Graduate Programs, Karabuk University.

Prof. Dr. Hasan SOLMAZ .....
Director of the Institute of Graduate Programs

"I declare that all the information within this thesis has been gathered and presented in accordance with academic regulations and ethical principles and I have according to the requirements of these regulations and principles cited all those which do not originate in this work as well."

Ahmed Saad Najm AL-GBURI

ABSTRACT

M. Sc. Thesis

THE INVESTIGATION OF BIODEGRADABLE CORROSION PROPERTIES OF HOT ROLLED AT31 MG ALLOYS

Ahmed Saad NAJM AL-GBURI

Karabük University
Institute of Graduate Programs
The Department of Metallurgical and Materials Engineering

Thesis Advisor:
Assist. Prof. Dr. İsmail Hakkı KARA
June 2022, 70 pages

Manufacturers in this period face many challenges in manufacturing lightweight and efficient materials. Magnesium is an excellent alternative material for this application for steel, aluminum-containing alloys, and polymers. On the other hand, the poor corrosion resistance of magnesium alloys limits their use in both industrial and medical applications. As a result, a deeper understanding of the underlying mechanisms and components that control the corrosion of magnesium is required, as well as better approaches to improving corrosion performance. The main material used in this study was AT31 Mg alloy. After casting, a 12-h heat treatment at 350 °C was used to homogenize the material. A hot rolling procedure was used to create the alloy Mg-2.5Al-1.0Sn-0.3Mn-0.4La-(0.16,0.66,1.33Gd). At speeds of 1.5 m/min, 4.7 m/min, and 10 m/min, the AT31 Mg alloy with varying amounts of Gd was subjected to 20% deformation on each pass. Each sample contains eight lanes in total. Several tests have been studied on magnesium alloys (AT31) such as the immersion test and

potentiodynamic test in magnesium alloy as well as scanning electron microscopy (SEM) of rolled, milled, polished and etched samples to study the resulting changes in the microstructure for all samples of Mg AT31.

Key Words : Mg alloys, rare earth metals, SEM, Hot rolling**.**
Science Code : 91501

ÖZET

Yüksek Lisans Tezi

THE INVESTIGATION OF BIODEGRADABLE CORROSION PROPERTIES OF HOT ROLLED AT31 MG ALLOYS

Ahmed Saad NAJM AL-GBURI

Karabük Üniversitesi
Lisansüstü Eğitim Enstitüsü
Metalurji ve Malzeme Mühendisliği Anabilim Dalı

Tez Danışmanı:
Dr. Öğr. Üyesi İsmail Hakkı KARA
Haziran 2022, 70 sayfa

Bu dönemde üreticiler, hafif ve verimli malzemeler üretmede birçok zorlukla karşı karşıyadır. Magnezyum, çelik, alüminyum içeren alaşımlar ve polimerlere bu uygulama için mükemmel bir alternatif malzemedir. Öte yandan, magnezyum alaşımlarının zayıf korozyon direnci, hem endüstriyel hem de tıbbi uygulamalarda kullanımını sınırlar. Sonuç olarak, magnezyumun korozyonunu kontrol eden temel mekanizmaların ve bileşenlerin daha derin bir şekilde anlaşılması ve ayrıca korozyon performansını iyileştirmek için daha iyi yaklaşımlar gereklidir. Bu çalışmada kullanılan ana malzeme AT31 Mg alaşımıdır. Dökümden sonra, malzemeyi homojenleştirmek için 350 °C'de 12 saatlik bir ısıl işlem kullanıldı. Mg-2.5Al-1.0Sn-0.3Mn-0.4La-(0.16,0.66.1.33Gd) alaşımını oluşturmak için bir sıcak haddeleme prosedürü kullanıldı. 1.5 m/dak, 4.7 m/dak ve 10 m/dak hızlarda, değişen miktarlarda Gd içeren AT31 Mg alaşımı her geçişte %20 deformasyona maruz bırakıldı. Her numune toplamda sekiz paso içermektedir. Magnezyum alaşımında daldırma testi ve

potansiyodinamik testinin yanı sıra haddelenmiş, zımparalanmış, parlatılmış ve dağlanmış numunelerin taramalı elektron mikroskobu (SEM) gibi magnezyum alaşımı (AT31) üzerinde çeşitli testler, hepsinin mikro yapısında ortaya çıkan değişiklikleri incelemek için incelenmiştir.

Anahtar Kelimeler : Mg alaşımları, nadir toprak metalleri, SEM, Sıcak haddeleme.
Bilim Kodu : 91501

ACKNOWLEDGMENT

At first and before everyone, I would like to thank God who helped me complete this study. Then I would like to express my thanks, appreciation, and respect to my family, especially my parents, who supported me morally and financially, without them, I wouldn't be where I am now. I would like to thank my friends who motivated me and helped me achieve this achievement. It is difficult to complete this thesis without the experience of my supervisor Assist. Prof. Dr. Ismail Hakkı KARA, whom I would like to thank for his support, assistance, and guidance to me, and I would like to thank the discussion committee for the long scientific time in studying this thesis and giving me some valuable advice and information.

In addition to, I would like to thank the KBU-BAP unit for supporting this study with BAP Project No: KBÜBAP-21-YL-101 by Karabuk University Scientific Research Projects Coordinator ship.

CONTENTS

Page

Page

Page

LIST OF FIGURES

Page

Page

LIST OF TABLES

Page

SYMBOLS AND ABBREVITIONS INDEX

SYMBOLS

Cl : Chlorine
Mg : Magnesium
Al : Aluminum
Sn : Tin
Zn : Zinc
Mn : Manganese
Gd : Gadolinium
La : Lanthanum
Ca : Calcium
Li : Lithium
Fe : Ferrous
Ni : Nickel
Ce : Cerium
Ta : Tantalum
Al2O3 : Alumina
A12 : Al12Mg17
HF : Hydrofluoric acid

ABBREVITIONS

GPA : Grade Point Average
FCC : Face Centered Cubic
MPa : Megapascal
HCP : Hexagonal Close-Packed
EDS : Energy Dispersive X-ray Spectroscopy
HCP : Hexagonal Close-Packed

RE : Rare earth elements

ASTM : American Society for Testing and Materials

MBM : Magnesium Based Materials

HBSS : Hank’s Balanced Salt Solution

Icorr : Corrosion current

Ecorr : Corrosion potential

Mpy : Miles per year

SEM : Scanning Electron Microscope

EDS : Scanning Electron Microscope

XRD : X-Ray Diffraction

SBF : Simulated Body Fluid

PART 1

INTRODUCTION

Currently, the scientific community places a great deal of emphasis on the development of magnesium alloys for use in biomedical applications. Compared to conventional metallic materials, plastics, and ceramics, magnesium alloys provide several advantages. Magnesium alloys, for instance, have a low density (1.74–2.0 g/cm3) and an elastic modulus of roughly 41–45 GPA. This is much smaller than the elastic modulus of other conventional metallic biomaterials, such as titanium alloys (110–117 GPA) and stainless steel (205–210 GPA), which is essential for avoiding stress shielding. Other conventional metallic biomaterials include alloys of zirconium (110–117 GPA). Due to their better mechanical properties and fracture toughness, magnesium alloys are preferred over polymers and ceramics for load-bearing applications. Magnesium is an essential mineral for human metabolism and other biological processes. This cation is the fourth most prevalent in the human body. The investigation of magnesium implanted in live beings shows significantly increased bone volume that has formed firmly around the magnesium, indicating that it biodegrades effectively. The development of magnesium alloys has facilitated the use of implants in both unloaded and loaded situations. These include, among others, biodegradable stents, screws, and intramedullary nails. Magnesium alloys are very reactive, resulting in an exceptionally high rate of corrosion (a highly negative standard electrode potential of 2.34 V). This is the most significant drawback of employing magnesium alloys as biomedical materials, despite their numerous advantageous features. Specifically, they corrode excessively quickly in solutions containing Cl, such as human body fluid or blood plasma. In particular, this is the case. Furthermore, magnesium alloys are sensitive to galvanic corrosion, which may rapidly degrade the material. To regulate the corrosion rate of magnesium alloys, it is vital to understand the relationship between the microstructure and the bio-corrosion rate. Zinc is widely acknowledged as both one of the most abundant and nutritionally significant

minerals present in the human body. Therefore, its usage in biological applications is without danger. Zinc is helpful because it helps to enhance the impurity tolerance limits, which boosts the magnesium alloys' corrosion resistance [1].

1.1. MAGNESIUM (Mg)

1.1.1. Description

Magnesium corresponds to the element with the chemical formula Mg and atomic number 12 on the periodic table. This element's native state is silver-colored. Due to the creation of an oxide layer (MgO) that prevents further corrosion, magnesium tends to oxidize and acquire a greyer color when exposed to air. This element is a member of the alkaline earth metals group. Due to its low density, it is extensively employed in the automotive and aerospace sectors as a component of light alloys. Magnesium exposed to air ignites in the presence of an ignition source, producing a powerful white flame. It is unwise to attempt to extinguish the flame by adding water since magnesium interacts aggressively with water vapor, producing hydrogen and increasing the flame's intensity. Mg_3N_2 is formed when magnesium combines with nitrogen in the air. Sand may be used to put out a magnesium fire [2].

1.1.2. General Properties

Magnesium (Mg) alloys are desirable structural materials for lightweight vehicles due to their low density and excellent strength-to-weight ratio. The extensive use of magnesium alloys in automobiles can reduce fuel consumption by means of lightweight, which is beneficial for the environment. Mg alloys are also considered to be promising biodegradable implants for usage within the human body. However, the low corrosion resistance of Mg alloys prevents their extensive use in both industrial and medicinal applications. Consequently, it is crucial to have a deeper understanding of the mechanisms and key elements that govern Mg corrosion and to develop more effective strategies for enhancing their corrosion resistance [3]. Fabricators working on production in this period are expected to face a variety of challenges when producing lightweight and efficient materials. Magnesium is the finest alternative for

developers in terms of production and manufacturing, and it may be utilized in place of materials like steel, aluminum alloys, and plastic. Because of its exorbitant cost, magnesium has received very little research and development attention in recent years. Magnesium is now being considered because the price of magnesium alloys has fallen in comparison to the past. The strength of magnesium alloys has been favored over other metals such as copper and aluminum-based alloys [4]. Casting is the most popular method for producing magnesium-based alloys, with 98 percent structural uses. Magnesium alloys are widely used in a range of industries, including the automotive, aerospace, and medical sectors, due to their low density, fine specific strength, and good damping capabilities. Magnesium alloys are substantially lighter than other alloys, such as aluminum alloys. Magnesium alloys also have a particularly strong strength-to-weight ratio, which is one of the reasons why material producers and engineers value them so highly. Magnesium alloys play a crucial role in the vehicle production business due to their high level of stiffness, high capacity to absorb vibrations, and excellent cutting capabilities [5].

1.2. ALLOYING ELEMENTS

1.2.1. Aluminum (Al)

Aluminum (Al), the third most prevalent element in the Earth's crust, occurs naturally with oxygen and other minerals. The third most frequent element is aluminum. Due to its face-centered cubic (FCC) form, it can be treated with relative ease and is ductile at room temperature. Compared to other technical metals, aluminum has a comparatively low melting point of around 660 degrees Celsius. Aluminum has a vast array of capabilities, qualities, and physical, chemical, and mechanical traits, which present themselves in a multitude of alloys. We may briefly discuss the most essential qualities of aluminum, such as its very low specific weight, which is around a third that of iron. It can be readily formed, rolled, drawn, extruded, and welded, making it the perfect building metal. Its elastic unit (70,000 MPa) is three times lower than iron's (200,000 MPa). The aluminum frame has three times the elastic elongation of the iron frame under load circumstances. Aluminum and the majority of its alloys are very resistant to a variety of kinds of corrosion. Due to its tight chemical affinity with

oxygen, the metal's surface is permanently coated with a coating of aluminum oxide, which is a very efficient method of preventing future corrosion. This feature makes them attractive in the building, maritime engineering, and transportation (cars, trains, and aircraft) industries [6]. Aluminum is the appropriate material because of its low specific gravity and near-zero maintenance costs. Aluminum is an excellent conductor of both heat and electricity. They cannot be magnetized or burnt, which is essential for a variety of applications, including electronics and offshore equipment (oil rigs). It is non-toxic when in contact with food (within a safe toxicity range) and appears as a protective film with extremely low permeability, qualities that make it the raw material for food packaging, especially multi-layer flexible packaging (e.g. polyester, aluminum, polyethylene). Low secondary heat emission factor and high diffusion reflectivity (whiteness). The Bayer process converts bauxite, from which aluminum may be mined, into alumina, or aluminum oxide. Typically, aluminum is derived from bauxite. The Bayer process, which has remained constant since its creation in Germany by Karl Josef Bayer in 1988, is used to process all of the alumina used by the market-based aluminum sector. The Hall-Hold method is used to produce the majority of aluminum. Since 1886, when Charles M. Hall and Paul L. Heroult were given the first copyrights in the United States and France, respectively [7], this method's fundamental features have not altered much. The previous studies have shown the secondary phase of Aluminum with Magnesium. However, Mg-Al phase Figure 1.1, includes the liquid phase, the HCP structured solid phase and the R phase. Al dissolves at most 18.9% (will be atomic) at 450 °C [8].

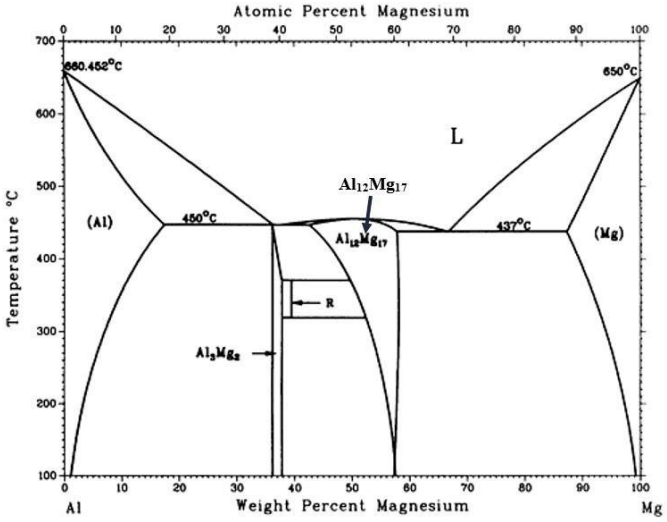

Figure 1.1. Mg-Al secondary phase diagram [9].

1.2.2. Tin (Sn)

Tin is a malleable, silvery-white, malleable metal. Because tin is covered with a layer of oxide, it does not oxidize quickly and is resistant to corrosion. Tin is resistant to corrosion by seawater and tap water but is susceptible to attack by strong acids, alkalis, and acidic salts. Tin, whether pure or ethereal, is a useful metal because of its poor thermal conductivity, low density, and low modulus of elasticity. Moderate strength Strong corrosion resistance in a variety of settings and a high degree of reactivity with a number of other elements. Tin can be found in 2 different forms, or allotropes: the familiar form, beta or white tin, and alpha or gray tin, which is powdered and of little use. Gray changes to white above 13.2 °C, rapidly at temperatures above 100 °C; The reverse metamorphism, called tin blighting, occurs at low temperatures and seriously hampers the use of the metal in extremely cold regions [10]. The crystal structure of an atom is a body-centered tetrapod. It exhibits allotropic properties in both its natural and mineral states. Its transformation is identical to the corrosion transformation because it acts as a handle for materials that possess a property known as the friability of the metal from it. This is the case because its main role is to change the metal. During the modification process, high-resolution scanning electron microscopy (SEM) was used so that researchers could assess the link created between allotropes [11,12]. The previous studies have shown the secondary phase of Tin (Sn) with Magnesium and their effect in the fusion temperature in Figure 1.2.

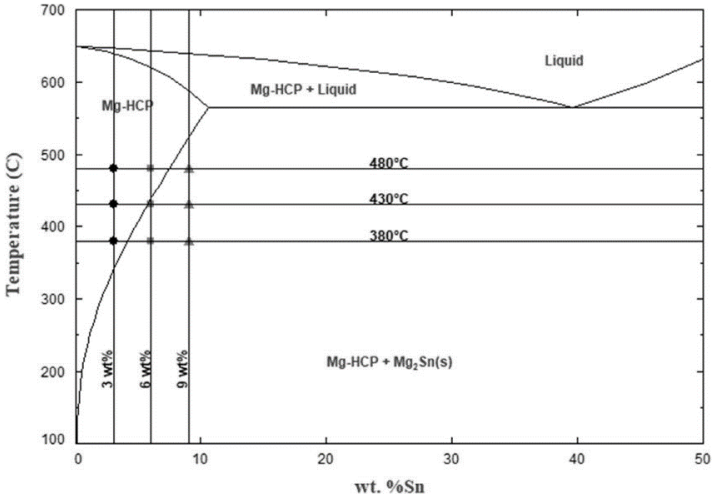

Figure 1.2. Mg-Sn secondary phase diagram [9].

1.2.3. Zinc (Zn)

Zinc is a metal with a relatively boiling point (907 °C) and low melting point (419.5 °C), ranking fourth behind iron, aluminum, and copper. Its unbranched strength and hardness are superior to those of tin and lead, but notably inferior to those of aluminum and copper. Due to its limited creep resistance, pure metal cannot be employed in demanding applications. Due to these factors, the vast majority of zinc applications include alloying or plating with iron or steel. Except when very pure, zinc is brittle at normal temperatures, but becomes pliable at around 100°C and may then be readily rolled; hence, unalloyed wrought iron is often used for zinc roofing with full support. However, the inclusion of modest amounts of copper and titanium considerably improves the creep resistance of coiled sheets, resulting in the material of rising industrial relevance for roofing [13]. The global zinc supply climbed to 13.4 million tons in contrast to the demand of 13.77 million tons [14]. The recycling technique has rendered a substantial quantity of zinc useable, and its output is estimated to be between 20 and 40 percent of the global total [15]. Approximately fifty percent of all zinc is used to galvanize steel and prevent corrosion. Recently, it was shown that zinc is a biodegradable mineral that can readily replace iron and magnesium [16]. Approximately 15 percent of the total quantity of zinc in the world is considered a base metal and is used to manufacture zinc-based alloys. On the market, zinc alloys are readily available as wrought ingots, drawn wire, applied extrusion, and forged

products. Recently, the most advanced zinc alloys for extrusion and forging have been produced and made commercially accessible [17]. The previous studies have shown the secondary phase of Zinc with Magnesium. However, MgZn2 phase dissolves at 595°C as it is shown in Figure1.3, this phase is in eutectic state at 97% Zn content at 368 °C. There are no solid melt regions in this system [8].

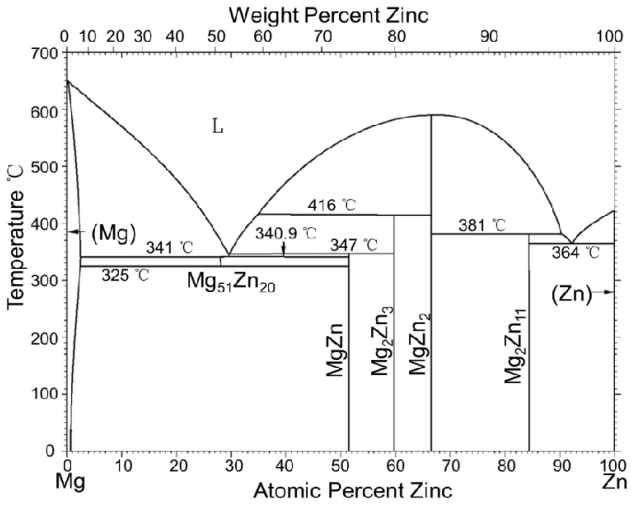

Figure 1.3. Mg-Zn secondary phase diagram [9].

1.2.4. Manganese (Mn)

Manganese (Mn) is a micronutrient required by the majority of organisms and is chemically active in pink. It is a brittle and very hard metal that is difficult to melt, but it oxidizes easily. Manganese reacts when it is pure, and as a powder, it reacts with oxygen and water (it rusts like iron) and dissolves in dilute acids. Manganese is necessary for the manufacture of iron and steel. Currently, 85% to 90% of total demand is met by the steel sector, which is the largest portion of total demand. Manganese is an important component of stainless-steel low-cost formulations and many widely used aluminum alloys. In addition, Manganese is used to decolor glass and produce violet glass [18]. South Africa is the world's largest producer of manganese, producing more than 82 percent of the world's total manganese [19]. We may use manganese-containing steel which is affordable and corrosion-resistant [20]. The previous studies have shown the secondary phase of Manganese with Magnesium. However, Mn

dissolves at 653 °C at the rate of 2% (will be atomic.). There is no intermediate composition in the Mg-Mn binary phase Figure 1.4, [8].

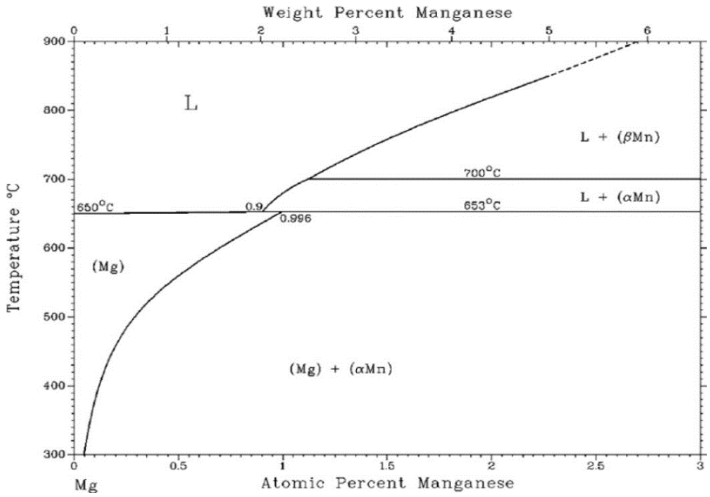

Figure 1.4. Mg-Mn secondary phase diagram [9].

1.3. RARE EARTH ELEMENTS

1.3.1. Gadolinium (Gd)

It is one of the rarest minerals on earth. It is a delicate, lustrous, silvery metal with semi-elastic properties. In the presence of moist air, gadolinium turns into a form of white oxide that protects it from oxidation. This element is highly soluble in dilute acids and reacts very slowly with colorless salts producing water. In compounds, the element occurs in its trivalent state. Gadolinium is ferromagnetic and has a stronger magnetic attraction than nickel at room temperature or as low as 20°C. the element's magnetism is at its peak. At high temperatures, this metal produces binary compounds containing nitrogen, sulfur, carbon, phosphorous, selenium, boron, silicon, and arsenic [21]. The majority of researchers in the field of materials have used gadolinium to enhance the properties of many alloys. It has been shown that the addition of rare earth elements such as Ce, La, Gd, and Nd to magnesium alloys enhances their resistance to corrosion and creep [22]. The rare earth metals are responsible for producing the inter-metal consolidation phase, which is very stable even at high temperatures, and the rare earth elements with high solubility are responsible for forming a solution in the -Mg matrix, a solid that provides magnesium and alloys that have great toughness [23].

After DE oxidation, gadolinium turns into a silvery-white metal. Gadolinium slowly combines with oxygen or moisture in the air to form a black covering. At this temperature, the element's magnetism is at its peak. It can only be found in nature in the oxidized form. Usually, it contains impurities of the rare earth when separated due because their similar chemical properties [24]. The previous studies have shown the secondary phase of Gadolinium with Magnesium. However, Mg dissolves at the eutectic temperature up to 23.49% (at % Gd) as it is shown in Figure 1.5, thus providing solid melt hardening [25].

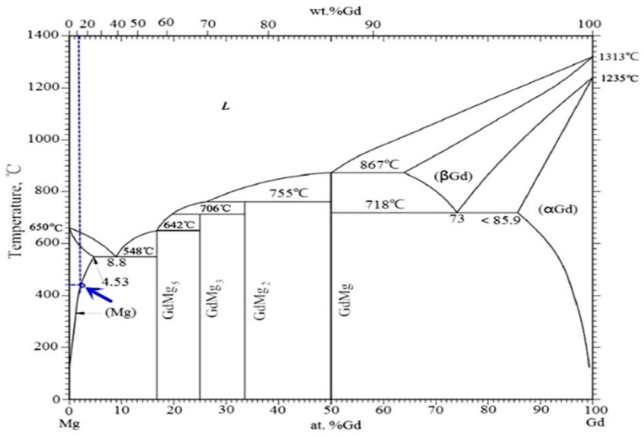

Figure 1.5. Mg-Gd secondary phase diagram [26].

1.3.2. Lanthanum (La)

Lanthanum is a malleable, silvery-white metal that can be cut with a knife. It is the second most reactive rare earth metal after europium. At room temperature, lanthanum is oxidized in air to produce La2O3. Due to the formation of a protective fluoride layer (LaF3) on the surface of the metal, it reacts slowly with water and quickly dissolves in dilute acids, with the exception of HF acid. The metal is magnetic from 6 K (267 °C) to its melting point at 1,191 K (918 °C), with magnetic sensitivity being practically temperature independent between 4 and 300 K (269 and 27) [27]. In most cases, adding rare earth elements such as lanthanum to magnesium, aluminum, and other alloys improves the performance of these alloys. These improvements include an increase in the alloy's durability as well as a reduction in its weight, resulting in an exceptionally lightweight material that is highly useful in product production [28]. The inclusion of rare earth metals increases the yield strength of magnesium alloys [29]. The previous

studies have shown the secondary phase of Lanthanum with Magnesium. However, La has very low solubility in Mg and has a very high eutectic temperature (612 °C) as it is shown in Figure 1.6. It does not improve its aging ability due to its low dissolution [25].

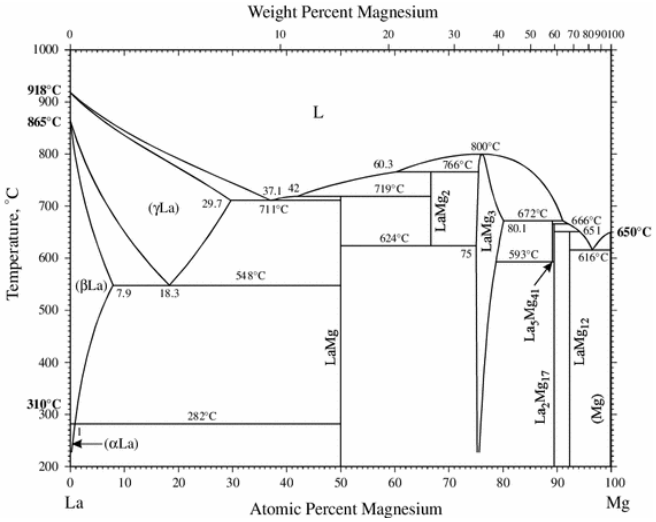

Figure 1.6. Mg-La secondary phase diagram [25].

1.4. APPLICATION OF MAGNESIUM ALLOYS

The military was the first to use magnesium alloys for their many applications. Currently, it has shifted to industries that need less energy use and less greenhouse gas emissions, most notably the automotive sector. The usage of magnesium alloys in automotive manufacturing dates all the way back to the 1920s. Due to the need for lightweight components in a range of sectors, particularly the automobile industry, researchers have concentrated on magnesium-aluminum alloys. This need has motivated researchers to discover uses for magnesium-aluminum alloys, such as the reduction of vehicle weight. In the United States, this technique was originally used on the engine pistons of a racing car used in the Indy 500. In 1937, close to 4 million Mg pistons were manufactured in Germany. The crankcase that incorporated the Mg component was first manufactured by the general engine in 1931. In the 1970s of the previous centuries, the car industry used air-cooled transmissions and engines. As a consequence of greater engine power and overheating, water-cooled engines began to replace air-cooled engines, and magnesium components began to be used less often.

Since 1990, firms like Mercedes and BMW have manufactured components to protect autos against scratches in a number of different ways. In addition, it is an ideal material for the production of any portable electronic device [30-31].

PART 2

LITERATURE REVIEW

2.1. MAGNESIUM ALLOYS

2.1.1. General Properties

Aluminum, beryllium, lithium, zinc, and other lanthanides are among the most common components used in the production of commercial magnesium alloys. The low density of this alloy is its distinguishing feature. These alloys, including carbon steel, aluminum alloys, and titanium alloys, are the lightest of all structural materials. In general, magnesium alloys can be divided into two main categories. The first group consists of metal alloys containing between 2 and 10 percent aluminum and combined with additional elements of a lower average proportion, including zinc and manganese. Even when heated to temperatures as low as -120 ° C, these alloys retain appropriate mechanical properties. The second group to be addressed is magnesium alloys that contain elements other than aluminum, including the rare earth elements, zinc, thorium, and silver. All of these magnesium alloys contain a trace amount of zirconium, although these other elements are also present. This component is necessary because it allows the production of a material with a reduced particle size, and as a result, the mechanical properties are enhanced. As a result of the use of more expensive alloying components, these alloys have greater mechanical properties at elevated temperatures, and their production requires specialized technologies. Thus, the cost of this alloy has increased. In addition to the above properties, magnesium alloys provide excellent machining properties, even at high cutting speeds. In addition, magnesium alloys can be welded in a protective environment (inert gases), as shown in Table 2.1. for the most commonly used alloys, which contain a major alloying element such as aluminum (AZ, AM, AS, AE, and AT series). Another advantage of magnesium alloy over other metal alloys is that its melting temperature is lower than

that of other metal alloys (between 650 and 680 °C, depending on the alloy), and it requires less energy to melt [32]. Magnesium alloys usually compete with polymers in a number of applications; However, it usually has a higher mechanical quality, stronger resistance to the effects of aging, enhanced electrical and thermal conductivity, and is easier to recycle than plastic. However, due to a variety of defects, this material cannot be exploited on a larger scale. The low malleability of magnesium and its alloys at room temperature is the root cause of the material's most important defects in terms of its mechanical properties. As a result, there are a limited number of skippable alloys that can be used. Thus, casting or hot working at temperatures between 200 and 350°C is the most efficient method for producing components. Chemically speaking, magnesium alloys are very brittle and susceptible to corrosion, especially in marine environments and this is especially true of magnesium. In contrast, the wear resistance is sufficient when exposed to normal atmospheres. Combined with poor creep resistance, these qualities preclude its employment in a range of applications with specific requirements. In addition, there have been some concerns that have been highlighted regarding the recycling of magnesium alloys. Even if the technical part of the equation is reduced, magnesium recovery circuits have not yet been installed in production units. Finally, there are some economic issues that need to be taken into consideration, namely the fact that there are few manufacturers which leads to an increase in the price of the final material [33].

Table 2.1. Common magnesium alloys and their applications [34].

Name of Mg Alloy	Alloy Elements	General Applications	Basic Properties and Applications
AZ91	9.0%Al 0.7%Zn 0.13%Mn	General purpose casting alloy	Good molding, good mechanical properties at T <150ºC
AM60	6.0%Al, 0.15%Mn	High pressure casting alloy	Higher toughness and ductility than AZ91, slightly lower strength. Often used in structural automotive applications
AM50	Mg-Al System	General purpose casting alloy	Good strength, ductility, energy absorption and molding properties.
AE44	Mg-Al rare earth system	General purpose casting alloy	Better deformation and molding behavior than AE42
AE42	Mg4 atomic percentage Al2 atomic percentage rare earth	General purpose casting alloy	Low molding level, good deformation behavior
AS41	4.2%Al, 1.0%Si	General purpose casting alloy	Better creep resistance than AZ91 at high temperatures but lower strength
ZE41	4.2% Zn, 1.2% Terras Raras, 0.7% Zr	special casting alloy	The addition of rare earths improves the deformation resistance at elevated temperatures. Strong pressure.
AZ31	3.0% Al, 1.0Zn, 0.2% Mn	forged magnesium products	Good alloy for extrusion
AM20	Mg-Al system	casting alloy	High ductility, toughness, poor molding
MRI 153M	Mg-Al-Ca-Sr system	casting alloy	For high temperature applications up to 150°C
MRI 230D	Mg-Al-Ca-Sr system	casting alloy	For high temperature applications up to 190°C
AS 21	Mg-Al-Si system	casting alloy	For use at temperatures above 120°C
AJ62	Mg-Al-Sr system	High pressure casting	Good thermal and mechanical resistance, superior casting, corrosion resistance and deformation behavior

2.1.2. Classification of Magnesium Alloys

There are a number of alternative coding and identification systems for magnesium alloys, but none of them have yet attained universal recognition. American Society for Testing and Materials-established terminology for non-ferrous metal alloys is used for the purposes of this research (ASTM). This nomenclature offers information on the

composition and heat treatment of the alloy. The American Society for Testing and Materials (ASTM) has its own classification system for magnesium alloys, and each magnesium alloy type has its own name. This method may be split into four parts: the first component of the classification consists of two letters denoting the two most important alloying elements. Table 2.2. [35] lists the most significant alloying elements, together with the letters used to identify them.

Table 2.2. Main alloying elements.

A: Aluminum	**B**: Bismuth	**C**: Copper	**D**: Cadmium	**E**: Rare Earths
F: Iron	**G**: Magnesium	**H**: Thorium	**K**: Zirconium	**L**: Lithium
M: Manganese	**N**: Nickel	**P**: Lead	**Q**: Silver	**R**: Chromium
S: Silicon	**T**: Tin	**W**: Yttrium	**Y**: Antimony	**Z**: Zinc

The second part of the classification consists of two digits that indicate the percentage of the two main alloying elements. The third part of the classification corresponds to a sequential letter, assigned by patent order, which allows the differentiation between alloys with the same content of alloy elements:

- A: First compositions, registered with ASTM
- B: Second compositions, registered with ASTM
- C: Third compositions, registered with ASTM
- D: High purity, registered with ASTM
- E: High corrosion resistance, registered with ASTM
- X: Experimental alloy, not registered with ASTM

Finally, the fourth part of this classification identifies the type of heat treatment or mechanic to which the alloy was subjected:

- F: As fabricated
- O: Annealed
- H: Strain hardened
- W: Solution heat treated
- H10 and H11: slightly hardened
- H23, H24, and H26: work-hardened and partially annealed

- T4: solubilization heat treatment
- T5: artificially aged
- T6: heat treatment of solubilization and artificially aged
- T8: solubilization heat treatment, cold worked, and artificially aged.

2.2. BIODEGREDABLE

The recovery of damaged tissue is expected to be aided by a special type of bioactive biomaterials known as degradable biomaterials, which will dissolve once the healing process is complete. The two types of metals that have been considered are magnesium-based alloys and iron-based alloys. Degradable biomaterials are especially focused on implants for the treatment of orthopedic, cardiovascular, and pediatric disorders. Biodegradable metals, in principle, should provide temporary support throughout the healing process and then gradually degrade afterward. This should be done until assistance is no longer required. Magnesium-based materials are ideal for use in therapeutical devices, especially in orthopedic and cardiovascular applications, because they can be biodegraded [36]. The capacity of a material to interact with biological tissues in the body without producing unacceptable damage is referred to as MBM biocompatibility. The material's ability to interact with biological tissues is used to assess this capability. From a biological point of view, human tissue can not only tolerate but also benefit from interactions with MBM implants by engaging in the appropriate reactions. The interaction between MBMs and organic tissue in vivo, on the other hand, has been demonstrated to generate behaviors not observed in vitro. When mg interacts with water in an aqueous environment, such as organic tissue or in vitro cell culture, it creates magnesium hydroxide (Mg (OH)2) and molecular hydrogen. These reactions occur in a watery environment (H2). Biological reactions of mg-based materials have been examined in vivo and in vitro. Following MBM implantation, tissue develops gas pockets containing varying amounts of hydrogen, oxygen, carbon dioxide, and/or nitrogen, as well as a high deposit of calcium phosphate (CA-P), which acts as a mineral layer between the tissue and the MBM implants, and an increase in the local PH of bodily fluid. In vivo, gas pockets do not format because they are retained by local tissue, while in vitro, there are no gas pockets because they are easily discharged. On the other hand, there are gas pockets in vivo.

Molecular hydrogen, on the other hand, is released into the environment, and cell adhesion activity on the surface of MBM implants shows that they are biocompatible. Because of MBM corrosion, H2 was discovered to be a potent antioxidant that is engaged in cell signaling and has a unique function in preventative and therapeutic applications. After H2 was recognized as possessing these qualities, this discovery was made. The inclusion of a magnesium layer can enhance osteoinductivity, hence enhancing the biocompatibility of magnesium alloys as bone regeneration materials. According to the Bohr effect, an increase in ph. correlates positively with hemoglobin's ability to absorb oxygen in the blood and negatively with cell-mediated bone resorption by rat osteoclasts in vitro [37].

2.2.1. Biodegradable Metal Implants

Biodegradable metal implants have been the subject of substantial research, primarily for orthopedic and cardiovascular applications. This was due to metals' greater mechanical properties when compared to biodegradable polymers. Metals that are innately biocompatible, such as Mg, Fe, and Zn, were obviously the focus of such research. When used as structural implants in vivo, however, it immediately became obvious that these metals had inherent limitations. Increased corrosion rates were seen in magnesium-based implants, which were accompanied by hydrogen gas evolution, which can lead to early mechanical integrity loss, tissue separation, and gas embolism. Iron-based implants that had acceptable corrosion rates accumulated many corrosive chemicals that were resistant to surrounding cells and did not appear to be digested or removed at significant rates. Zinc-based implants have weak mechanical properties and low corrosion rates, which could lead to fibrous encapsulation and significantly limit biodegradability. Given their limitations, this special issue focuses on the most recent scientific advances in developing biodegradable metal-based systems, with an emphasis on them in vivo safety performance. Biodegradable metals in the orthopedic industry, magnesium (Mg) alloys have been promised for biomedical implants, but their quick corrosion rate and mode provide a clinical concern. To push Mg alloy materials into practice, a composite coating with high compatible components and biodegradable is created and produced to boost the anticorrosion property of an Mg alloy (i.e., AT31). The inner layer of Mg (OH)2 is micro-Nano structured after

hydrothermal treatment. Then, stearic acid (Sa) is added to change Mg (OH)2 in order to better close the gap beneath a polyethylene glycol surface-degradation polymer layer (1,3-trimethylene carbonate), By boosting adhesion strength at the interface between the outer and inner layers, this sandwiched coating, which benefits from the Sa modification effect, limits corrosive media penetration. The composite coating modified AZ31 outperforms the bare AZ31 in terms of anticorrosion and biocompatibility in both in vitro and in vivo testing. Surprisingly, the amount of newly created bone surrounding the composite coating modified implant has increased 1.7-fold after 12 weeks of implantation. The sandwiched biocompatible coating approach paves the way for future clinic translational applications of Mg alloys orthopedic materials [37].

2.3. HOT ROLLING DEFORMATION

Hot rolling is a metal deformation process that reduces the thickness of metal as it passes through a pair of rolls. Hot rolling is used to uniformly thin the specimen and impart the necessary and useful qualities to the material being rolled between the rolls. Fabrication of materials by hot rolling has been a big problem, and much work has been done on it recently. Artificial intelligence approaches are being used for it in both theoretical and practical ways [38]. The rolling process is one of the most popular in the manufacturing industry, with over 80% of metallic equipment having been exposed to it at least once throughout its production cycle. Flat rolling is the most practical of all the rolling procedures. This type of rolling is used to manufacture 40–60% of rolling products in industrial countries [39]. Hot rolling procedures are regarded as a significant method of producing semi-finished and finished goods such as rods, plates, and strips. The initial stage of this procedure involves heating the material in the hot deformation region to improve material workability and lower deforming metal flow stress. The metal is then plastically deformed in several rolling passes, which are common in roughing and finishing mills, to create the dimensions and desired shape. strain, Temperature, and strain rate distributions within the rolled metal play an important role in the kinetics of metallurgical events such as dynamic, meta-dynamic, and static recrystallization after or during hot rolling, as well as breakdown, during the process. As a result, the importance of understanding micro parameters and their

influences on metallurgical phase transformations through hot rolling process has always been emphasized, and numerous studies have been conducted to predict rolling process parameters as well as estimate the interconnection of micro parameters and the kinetics of static and dynamic metallurgical phase transformations [40].

2.4. CORROSION PROCESS

The definition of the term "corrosion" is a difficult issue since the variety of meanings connected with the phrase is continually expanding. The following definition has been identified as one of the most useful in the scientific literature: [41] "Corrosion is the deterioration of a substance (usually a metal) or its properties due to its contact with its environment." This term not only includes non-metallic materials such as ceramics, polymers, and natural materials, but it also refers to corrosion as a change in properties after the materials themselves have deteriorated, which is a very broad definition. Explain that classifications based on the concept of degradation do not include all events involved with corrosion, especially those linked with the corrosion of metals [42]. In some instances, the formation of an oxide coating on the surface of metals under particular conditions acts as a kind of protection against the material's deterioration. This clearly exemplifies this phenomenon. In this regard, a definition based on the concepts of interaction between matter and the environment with which it interacts may be more appropriate.

2.5. TYPES OF CORROSION

Depending on variables such as the kind of metal involved, the nature of the corrosive environment, the geometry of the structure, etc., the presence of corrosion may manifest itself in a number of ways. In most situations, the various forms of corrosive assaults are classified based on the appearance of the alloy surface [43]. This section is intended to offer an overview of the different kinds of corrosion failure processes, with an emphasis on those that most often affect magnesium and magnesium alloys. Consequently, we will refer to the following types of corrosion:

2.5.1. Galvanic Corrosion

The most prevalent and harmful type of corrosion is galvanic corrosion. Due to their negative corrosion potential, magnesium alloys operate as anodes when coupled with other technical metals. The voltage difference between the anode and cathode is the most critical component in galvanic corrosion. Another key component is anodic and cathodic polarization resistance. In an aqueous solution, Fe, Ni, Co, Cu, W, Ag, and Au act nobler than Mg alloy. Steel and aluminum, respectively, are the most and least damaging for Mg alloys used with aluminum, steel, and occasionally copper. Furthermore, Mg alloys can cause galvanic corrosion on their own. Depending on the micro-scale composition, microstructure, and crystal orientations, electrochemical activities result in the creation of galvanic pairs. The phase or composition of the anode or cathode might vary at this point. The particles in the Mg alloy, on the other hand, operate as micro anodes because they contain trace amounts of alloys as secondary phases, intermetallic, and impregnated particles [44]. Figure 2.1. shows galvanic corrosion on Mg alloy.

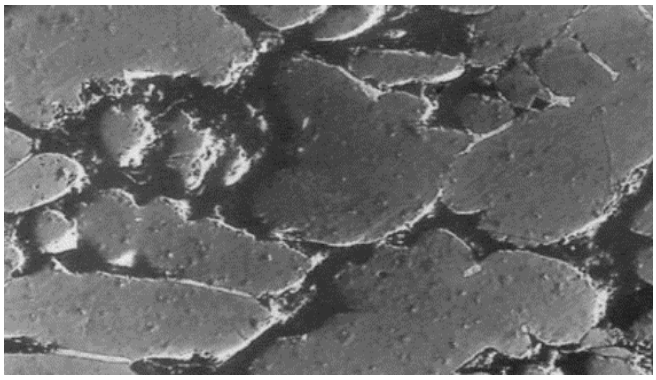

Figure 2.1. Galvanic corrosion of Mg alloys [45].

2.5.2. Uniform Corrosion

One of the secondary consequences of dissolution is the disappearance of a continuous layer of atoms from the surface. During this process, the anodes and cathodes are randomly distributed throughout the surface of the material, and their locations are

constantly altered. The wear form is responsible for the highest amount of mass loss, but because the attack is so constant, it is feasible to accurately predict how long exposed components or sections will endure. On the other hand, it is a kind of corrosion that, via its detection, can generally repair structures before structural hazards arise, and it is also a type of corrosion that can be easily controlled by the employment of preventive measures [46]. Figure 2.2. example of a uniformly corroded surface.

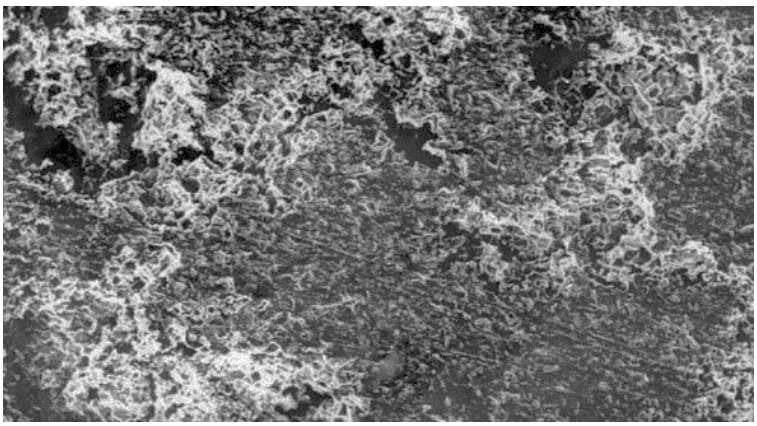

Figure 2.2. Uniform corrosion of Mg alloys [45].

2.5.3. Pit Corrosion

One of the distinguishing features of erosive pitting is the attack of erosion on a small area, which takes the form of a pinprick. This kind of corrosion begins at a weak point in the oxide layer and is amplified by the presence of aggressive anions, such as the chloride ions present in seawater. As a consequence of redox processes that increase the local acidity of the medium, the stomach grows. This stops the layer from reforming at the affected location. Due to its characteristics, the sting develops rapidly during its early phases but then drastically slows down as it continues to mature. The pits might be open or partially filled by a layer of corrosion products (the crust). This kind of pit erosion is induced by magnesium alloys with a heterogeneous crystal structure that includes the secondary phase Mg17Al12. There is an electrical exchange between the secondary phases, which have higher standard voltages, and the surrounding Mg matrix. The morphology of erosion often resembles holes. Feng et al. performed research to assess the effect of secondary phases on the corrosion resistance of AZ series magnesium alloys. According to the results of the study, secondary phases

may form both inside grains and along grain boundaries. These later phases perform the role of micro-cathodes. According to this notion, doing so will accelerate the breakdown of magnesium. According to [47], the most efficient phase of Mg17Al12 is the second phase. The significance of secondary stages in crater formation was shown by studies undertaken by Song and colleagues. It is well known that magnesium alloys with a larger amount of aluminum have stronger corrosion resistance than magnesium alloys with rare earth elements. During the search, deep holes were created, and the solubilization of secondary phases occurred first, followed by the melting of the magnesium matrix surrounding the secondary phases, and then the onset of the solubilization of secondary phases [48]. Figure 2.3. depicts the pitting corrosion found on the magnesium alloy.

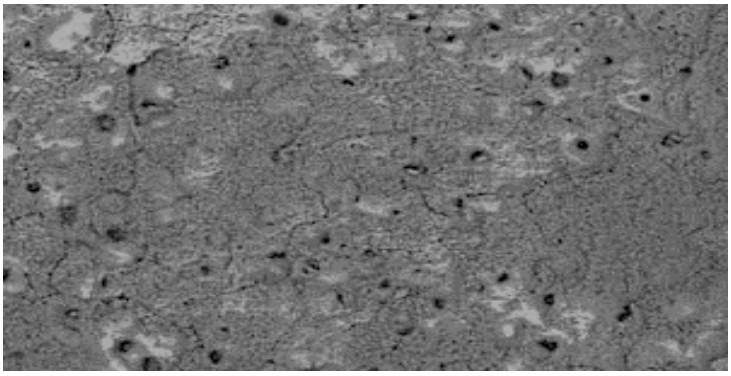

Figure 2.3. Pit corrosion of Mg alloys [45].

2.5.4. Intergranular Corrosion (IGC)

Granular erosion is an erosion associated with the separation of impurities or a second stage at the grain boundaries. This mechanism is associated with intergranular erosion events. The alloy becomes more susceptible to corrosion due to the depletion of these second-stage components in regions close to the grain boundaries. It is essential to note that localized corrosion, including interstitial corrosion, pitting, galvanic corrosion, and intergranular corrosion, poses a greater risk than general corrosion as it is more difficult to predict and detect. Despite the fact that in these types of attacks the collective losses are often very low, the depth of the attack causes a component to fail much sooner than expected [49]. Figure 2.4. shows intergranular corrosion on a magnesium alloy.

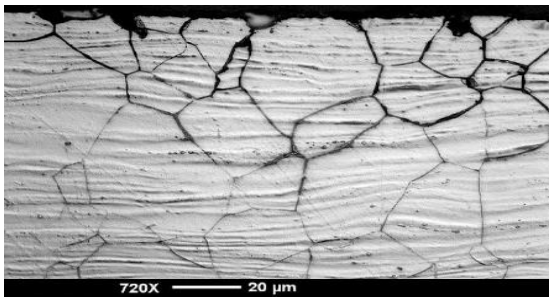

Figure 2.4. (IGC) of Mg alloys [49].

2.5.5. Filiform Corrosion

Filiform corrosion is one of corrosion type that occurs on metal surfaces. Paint, for example. Filiform corrosion is caused by galvanic cells that are active on protective metal surfaces. It spreads as a filiform in the early stages after hole-shaped corrosion, depending on the oxygen density on the surface [50]. Figure 2.5. shows filiform corrosion on Mg alloy.

Figure 2.5. Filiform corrosion of Mg alloys [50].

2.5.6. Stress Corrosion Cracking (SCC)

Another form of localized erosion is fissure erosion, which occurs in sheltered areas where oxygen is difficult to replenish. This type of corrosion is common in many metals and alloys, as is pitting corrosion. Creeping erosion and pitting erosion share many aspects in common, but on the other hand, there are differences between the two processes. Both generally involve the passive state, but pitting corrosion requires the presence of aggressive anions, while in slit corrosion this state is not necessary, although it accelerates the phenomenon and is present in most cases. Stress corrosion

occurs in extruded and extruded magnesium alloys, as well as fast-cooled cast alloys Creep corrosion occurs more easily than pitting corrosion. This is evidenced by the fact that in a given electrolyte, the alloy is activated more quickly in the gap than in the exposed region. This activation of metals in the vacuoles generally requires less potential than is necessary for pitting corrosion [51]. Figure 2.6. shows stress corrosion cracking on Mg alloy.

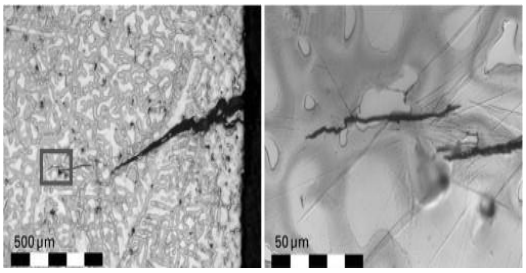

Figure 2.6. (SCC) of Mg alloys [51].

2.6. THE ELECTROCHEMICAL NATURE OF CORROSION

The great majority of corrosion processes in metals are caused by electrochemical reactions at the metal's surface. For the electrochemical process to occur, four primary conditions must exist [52]:

- Anode (Where oxidation or oxidation process occurs where a metal atom is oxidized and passed into a solution in the form of a positive ion leaving electrons on the surface of the metal).
- The cathode (or the cathodic reaction which consumes the electrons released in the anodic reaction, by reducing the species present in the aggressive medium).
- electrolyte (the immersion solution responsible for transporting ionic species to and from the metal surface).
- An electronic circuit (to connect the electrons produced in the anodic reaction).

From the foregoing, it can be concluded that if the metal has the ability to corrode, corrosion will not occur unless the anodic and cathodic processes occur simultaneously, with the same number of electrons generated by the anodic reaction (oxidation) consumed by the cathodic reaction. This is the only way that corrosion can

occur in metal with the possibility of corrosion. (reduction), depending on the absence of obstacles to the movement of electrons or ions. Oxidation and reduction in current density must be equal, leading to the compromise that neither state can exist independently of the other. This is one of the basic ideas of corrosion [53].

2.7. CORROSION IN THE ALLOYS OF MAGNESIUM

For several decades, magnesium alloys have had a bad reputation for corrosion, especially in saltwater environments. But the introduction of high-purity alloys in the 1980s dramatically changed the paradigm, providing one of the many catalysts that led to the emergence of high-pressure casting in the 1990s. Alloys containing novel materials that reduce heavy metal contaminants provide corrosion behavior in salt water that is consistent and competitive with aluminum alloys common in automobiles. The behavior of this alloy should be 2-3 times greater than that of its predecessors when tested in accelerated tests or when exposed to road salt. The following presentation summarizes the requirements for achieving optimal performance of magnesium alloys in corrosive environments. Factors include alloy composition, contaminants, model of manufacture, microstructure, and surface quality [54]. (1) The metallic factors affecting the corrosion behavior of the magnesium alloy structure are the composition of the alloy and its microstructure. In the composition of the alloy, the content of alloying elements as well as the presence of contaminants must be taken into account. Magnesium is anodic in relation to most other metals, so the development of fine piles between magnesium and alloying elements or impurities is an issue to consider. (2) Effect of some elements on the corrosion behavior of magnesium in salt solution, the elements such as aluminum, manganese, sodium, silicon, lead, and tin do not have a detrimental effect on the corrosion resistance of magnesium when present at up to 5% [18]. On the other hand, the presence of calcium, silver, and zinc accelerates the rate of corrosion, and this effect is more for iron, nickel, cobalt, and copper which have been shown to have very severe effects that are accelerated. Eat. The reason for this is that these elements act as cathodic sites, are active in reducing water, and sacrifice magnesium. In order to obtain good corrosion performance from magnesium alloys, the most common pollutants - nickel, copper, and iron - must be controlled so that they are present at low levels. Zirconium-

Magnesium Alloys The family of magnesium-zirconium alloys should be able to provide a corrosion behavior similar to that of the high-purity aluminum-magnesium alloys discussed above. However, many of these alloys contain zinc or silver at levels that moderate the corrosion of magnesium. The zirconium alloy family is typically used in low-pressure sand casting or permanent die casting applications. None of the alloys are considered high-pressure castings, and for this reason, they have not been involved in the recent increase in magnesium applications in the automotive industry. The yttrium-containing zirconium-based alloy and rare earth, WE54 and WE43, showed a corrosion resistance equivalent to that of high-purity aluminum alloys [55]. These modern alloys are alloys with improved composition, with strict limits on the most common contaminants, ensuring better corrosion resistance in aggressive media such as saline media. However, due to the high cost of yttrium, the use of this alloy is limited to the aerospace industry or other applications where weight is critical and where good mechanical properties at high temperatures are required. (3) Effects of granulators purifying grains with the addition of Zr are highly effective and are in fact the most efficient grain purification additives reported in metal alloys. Observation of the granule structure after casting the ingot into sand or permanent mold reveals spherical granules, the dimensions of which are characterized by the rate of cooling. It is generally possible to achieve particle sizes in the 10-100 μm range, depending on the cooling conditions. The effect of Zr on the sizing of pure magnesium grains and the consequent increase in mechanical strength (rupture and yield strength) and ductility. Various alloys, depending on the grain refining process, were developed by Zr. The possible mechanism is that Zr-containing elementary particles are formed in the foundry alloy. These intermetallic particles have a crystal structure that serves as a strong substrate for α-Mg growth, through the Liq + MgZr → α-Mg architectural interaction. Zr is compatible with various alloying elements such as Zn, Ag, Nd, Ce, Y, Th, etc. [56].

2.8. COMMON CAUSES FOR CORROSION FAILURE

Contamination during the melting and casting operations, as well as surface contamination during subsequent processes, contribute to the corrosion failure of high purity magnesium alloys [57]. Below are some of the most prevalent causes:

2.8.1. Sources of Indoor Air Contamination

- Iron contamination (die casting, sand casting, permanent die casting) Iron contamination of high purity aluminum alloys is often a concern during the first stages of production. In magnesium smelting, the use of fresh or clean troughs and conveying equipment promotes iron contamination. The manganese component of the alloy prevents contamination within the alloy's typical limits under normal conditions. However, equipment issues often emerge during startup, resulting in delays that might cause excessive emissions. In iron contamination, the melting temperature must also be addressed in addition to the aforementioned parameters. The contamination rate is greater the higher the temperature utilized.
- Nickel contamination (die casting, sand casting or permanent die casting) When steel containing nickel is submerged in molten magnesium, nickel contaminates the molten metal. Some chromium-carbon steels may be used safely for magnesium smelting, however nickel-containing alloy steels should be avoided.
- Copper contamination (die casting, sand casting, permanent mold casting) Aluminum alloys are the most prevalent source of copper contamination in foundries. The aluminum alloy has a significant quantity of copper, and the magnesium solubility may easily surpass the specified limit. To lessen the likelihood of these issues, it is customary to undertake aluminum smelting procedures independently from magnesium smelting methods. In their molten condition, magnesium alloys react with the oxygen in the air. During the process of magnesium smelting and purification, the surface of the molten metal must be shielded to avoid oxidation. Various fluxes of sulfur dioxide or sulfur hexafluoride are used for this purpose. In order to prevent oxidation and excessive molten combustion in a blast furnace, magnesium alloys were treated with molten salts until the early 1970s [58].

2.8.2. Sources of Surface Contamination

- Blowing Residues (Casting, Sand) Parts are often blown to improve appearance uniformity, polishing lines, and “clean” or polished surfaces.

- Heat treatment (low-pressure casting) - T4 and T6 heat treatments are sometimes performed in protective atmospheres of CO2 or CO2 + SF6 / SO2. Carbon pollution is accelerated at higher temperatures due to interactions with ambient carbon dioxide. However, the rate of erosion is not as severe as it would be if detonation residues were present. Mechanical or chemical cleaning may restore excellent wear resistance and surface cleanliness.
- Contaminants on the surface of the mold (mold casting) - The wear behavior of materials cast in a mold is often very diverse, depending on the history of the mold and the technology of lubrication of the mold. Even with a small amount of lubricant, it is possible to produce surfaces with a very uniform appearance, few signs of metal flux, and a low tendency to stick. However, test results indicate that sometimes more attractive surfaces are more susceptible to corrosion, presumably due to higher iron contamination on the mold surface. This surface contamination must subsequently be removed by mechanical or chemical cleaning to provide excellent corrosion resistance.
- Contaminants from water used to dilute matrix lubricant (die-casting) - Potable water should not be used to dilute lubricant without water quality regulation.
- Incompatible lubricants (die casting / forged dies) - Avoid graphite lubricants.
- Surface procedures (all types of metals) - Paint primers should be selected taking into account the compatibility of magnesium. Avoid the use of nickel and copper salts, but iron phosphate is useful and compatible with the pre-treatment of the coating. Low pH treatments should only be used on previously cleaned surfaces.
- Welding (low-pressure cast / ferritic goods) - Welding materials must be carefully selected to ensure purity compatible with the alloys used; However, the high temperatures used may leave cathodic impurities on the surface. New welding procedures and techniques must be thoroughly studied, not only for their mechanical strength but also for their potential impact on the surface quality of the affected area. Cathodic contamination in the weld metal may be of greater concern than surface contamination. To reduce the possibility of stress corrosion cracking failure, all welds should be discarded [59-60].

2.8.3. Cleaning Surfaces

- Surface cleaning and preparation techniques for dealing with the aforementioned sources of contamination are generally identical to those used for other metals. Among them are mechanical and chemical operations using solvents, alkaline baths, and acid treatments [61]. Despite the potentially severe impacts of shot blasting, magnesium components are often shot-blasted without repercussions by using an acid remover to eliminate surface contamination [62]. A pot scraping or vibrating technique with ceramic material and a washing solution is a successful mechanical cleaning method for castings. When appropriate media are utilized, there is no danger of residual contamination with this approach. In the case of aluminum-magnesium alloys that have not been cleaned by abrasive treatment, it is crucial that the chemical cleaning of the part utilizes both alkaline and acid treatments to ensure that the surface of the component is thoroughly clean. Adding surfactants to commercial phosphates may improve the cleaning of tiny quantities of process oil lubricants [63].

2.9. EFFECTS OF ALLOY ELEMENTS ON CORROSION BEHAVIOR OF MG

Metal loss occurs as the Mg17Al12 secondary phase grows, and stress corrosion cracks appear more often. Up to 5% in Minnesota (wt.) Mn has a negligible effect on corrosion resistance in pure Mg. Secondary phases of the Al_8Mn_5, Al6Mn and Al_4Mn types contribute to corrosion resistance in MgAl-Zn alloys. Impregnated elements like Fe are taken from the structure Zn; it is well known that MgxZny type secondary phases reduce Mg corrosion resistance due to local cathodic activity. Nd; Compared to pure Mg, Mg_3Nd is generated in binary Mg-Nd alloys and has a more effective cathodic action. As a result, it functions as a local cathodic zone, leaving a rising cathodic impact as the amount of Nd increases. Despite this, compared to La and Ce, it causes less metal loss. It also differs from $Mg_{12}Ce$ and $Mg_{12}La$ in that it has a larger atomic percentage [64]. By forming secondary phases of type Al-Nd and Al-Mn-Nd, the Nd element improves the corrosion resistance of the AZ series Mg alloys. The creation of a surface film is another contribution, but little research has been done on

this topic. Mg alloys' influence on corrosion resistance is still unknown. Secondary phases of Al_2Gd and Al-MnGd occur in Mg-Al alloys. The volume percentage of the secondary phase $Mg_{17}Al_{12}$ falls when Al is consumed. This scenario appears to have some influence on minimizing cathodic responses. However, corrosion behavior remains a mystery due to the heterogeneous microstructure and decreasing Al concentration of Gd-added Mg alloys. Long-term tests could be useful in determining the situation [64]. The effect of twinning on the corrosion properties of Mg alloy, which contains rare earth elements, was investigated by Liu et al. Y, Gd, and Nd. Micro-galvanic corrosion is said to occur between the twin and the matrix, resulting in quicker Mg dissolution and the creation of a surface layer. Under 26 extended immersion test conditions, the interplay of twin and surface layers is reported to boost the alloy's corrosion resistance [65]. Wan et al. investigated how ultra-fine grains affect the MGd-Y-Zr alloy's corrosion resistance. MgO films with extremely small grains have been reported to be more durable on the surface, leading to corrosion resistance. The oxide clings to the tighter surface because of the increased grain boundaries. Yang et al. looked into the influence of Ca on the corrosion resistance of Mg-Al-Mn alloys. It has been reported that when the percent Ca increases, the grains narrow, however in the first case, this occurs after the corrosion resistance decreases. With the addition of 2% Ca (Mg, Al), the 2Ca phase is claimed to be discontinuously scattered at the grain boundaries, giving this alloy the strongest corrosion resistance. These secondary phases act self-sacrificing in this situation, delaying Mg corrosion [66]. Y; Baek et al. studied the effect of Y addition on the corrosion resistance of Mg-Al-Ca alloys. With the addition of Y, corrosion resistance is reported to develop, with secondary phases containing Al being replaced by new phases such as Al_2Y. La; Because Al-La containing leafy secondary phases make the $Mg_{17}Al_{12}$ secondary phase more spherical and continuously diffused, La improves the corrosion behavior of Mg-Al alloys. This also results in a thinner microstructure and a thicker anti-corrosion film layer [67].

2.10. WAYS TO REDUCE CORROSION

In order to attenuate the corrosion of magnesium-based materials in order to enhance their service performance and expand their application range, it is necessary to create methods for reducing/preventing corrosion. Listed below are some of the known and confirmed corrosion prevention methods [68].

- Utilization of surface modification technologies, including laser annealing and ion implantation.
- Application of protective coatings and films to provide a barrier between the magnesium-based material and the environment.
- Utilize high-purity alloys and reduce impurity levels below their acceptable tolerance limits.
- Create novel magnesium-based materials by including additional alloying elements, reinforcements, or secondary phases.

Coating the base material is one of the most reliable and effective ways to prevent corrosion. To achieve adequate protection against corrosion, the coating layer must be characterized as follows

- Adhere well to the base material,
- Be free from pores,
- Be uniform, and
- Possess self-healing capability for applications where physical damage to the coating may occur [68].

2.11. HOMOGENIZATION AND HEAT TREATMENT

Due to their low density, high specific strength, good dimensional stability, and recyclability, magnesium alloys are gaining importance. As the lightest material for structural purposes, magnesium alloy is a possible replacement for steel and aluminum alloys. In recent years, research and applications on magnesium alloys have grown. Due to the restricted ductility of the hexagonal packed structure (HCP), the majority

of magnesium alloy products are now produced by industrial casting or semi-rigid forming, while plastic work processing is seldom employed. Mg and its alloys deform mostly through basal sliding and twinning at room temperature, which restricts their formability. Consequently, thermomechanical treatment is often carried out at elevated temperatures. Generally, it is believed that additional (prismatic and hierarchical) slip systems contribute considerably to deformation when the temperature exceeds 300 °C and the related critical shear stresses are equivalent. Nevertheless, it has been claimed that twinning may continue to operate even at high temperatures. Increasing interest in the utilization of magnesium in the transportation sector to enhance fuel economy by lowering vehicle weight has led researchers to concentrate on enhancing the plastic formability of magnesium. HSIANG and KUO evaluated the mechanical characteristics of hot-extruded AZ31 and AZ61 magnesium alloys under optimum processing conditions. YU et al. presented the stress curve of AZ31 alloy obtained at various strain rates and temperatures and determined the alloy's constitutive relationship. NODA et al. [69] examined the transition of the deformation mechanism of AZ31 alloy under high-temperature uniaxial tensile deformation and concluded that grain boundary slip dominated the stable deformation behavior. However, the microstructural development of AZ91 magnesium alloy remains mostly unexplored. Atoms diffuse across a concentration gradient as part of the homogenization procedure. Atoms diffuse in both directions, i.e., from the nucleus to the dendrite's surface and vice versa. Atomic diffusion is initiated by temperature and grows exponentially as the temperature rises. The shorter the homogenization time will be, the greater the temperature. Due to the fact that the dispersion of atoms differs across alloys, the time and temperature necessary for homogenization depend on the kind of alloy. In addition, the degree of separation and grain size in the casting change for both factors. Materials having a high tin and bronze content (more than 8 percent Sn) are notorious for their severe separation. In tin (phosphorous) bronze, silicon bronze, and copper-nickel alloys, diffusion and homogenization are slower and more difficult than in the majority of other copper alloys. Consequently, these alloys are often treated to a lengthy homogenization process. In these alloys, homogenization temperatures are typically maintained 50 °C below the solid's temperature, and soaking times vary from 3 to 10 hours [70].

PART 3

EXPERIMENTAL STUDIES

3.1. MATERIALS

In this study, AT31 Mg alloy and modified AT31 Mg alloy were used as primary and main materials. Table 3.1. lists the raw rolls that were used in the production process. Turkey was the source of pure magnesium, pure aluminum, and pure tin, while China was responsible for supplying the main alloys. For the manufacturing process, a technique known as low-pressure permanent die casting with a custom-made die was used Figure 3.1. and the casting conditions shown in Table 3.2. were strictly adhered to. Next, pure magnesium was placed in a stainless-steel crucible. When the temperature reached 775°C, there was an hour waiting period. Then, pure aluminum and then the main alloy was put into the crucible to finish the process. During this time, the liquid metal inside the vase was constantly being mixed by stirring. After the last edition of the ingot to a crucible made of pure tin, the temperature of the molten metal was measured to be 350°C while the pressure was between 2 and 3 atmospheres. The molds were then heated to a high temperature before the stainless-steel metal was injected into them. The chemical contents of the produced alloys are shown in Table 3.3. The Rigaku ZSX Primus II of the XRF Laboratory of the Iron and Steel Institute of Karabuk University was used for the chemical analysis process.

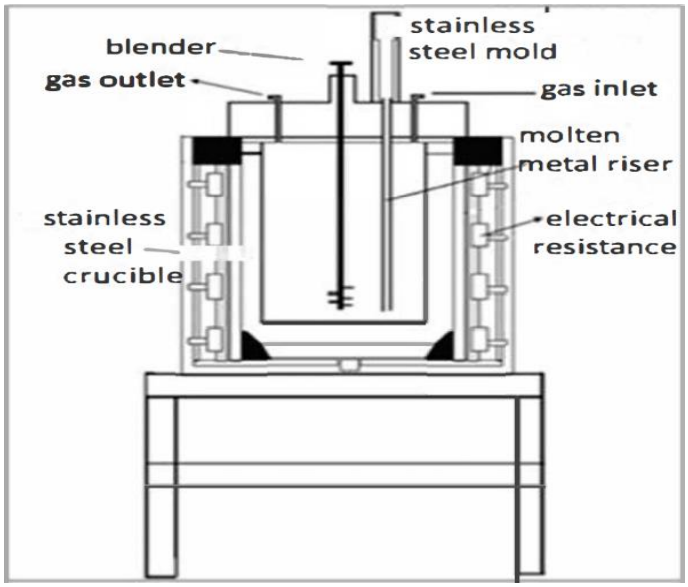

Figure 3.1. Diagram of low pressure permanent mold casting furnace.

Table 3.1. Casting conditions.

Shielding gas	Melting Temp (°C) standby Time (minutes)	Mold Temperature (°C)	Runner Temperature (°C)	Casting gaz pressure (atm)
Argon	775-60	350	350	2-3

Table 3.2. Production of Raw materials (weight in percentage).

Raw Material	Mg	Al	Sn	Mn	La	Gd
Pure Mg	%99,9	-	-	-	-	-
Pure Al	-	%99,9	-	-	-	-
Pure Sn	-	-	%99,9	-	-	-
Guage Mn	%90	-	-	%10	-	-
Guage La	%70	-	-	-	%30	-
Guage Gd	%75	-	-	-	-	%25

Table 3.3. Produced alloy groups (%).

Alloys Group	Mg	Al	Sn	Mn	La	Gd	Abbrevations
Mg-2.53Al-1.04Sn-0.3Mn-0.4La-0.16Gd	Bal.	2.53	1.04	0.37	0.36	0.16	A
Mg-2.4Al-1.03Sn-0.3Mn-0.4La-0.66Gd	Bal.	2.4	1.03	0.31	0.41	0.66	B
Mg-2.4Al-0.99Sn-0.3Mn-0.4La-1.33Gd	Bal.	2.4	0.99	0.35	0.39	1.33	C

3.2. HANK's BALANCED SALT SOLUTION (HBSS)

Isotonic buffer solution for carbohydrates and energy is known by the acronym HBSS, which stands for Hanks balanced salt solution. It is used in short cell culture, cell washing before dissociation, as well as in the transfer of cells or tissues. Calcium and magnesium are potential components of HBSS. Phenol red may also be present. HBSS is created by combining a basic powdered medium with water of appropriate quality for tissue culture. Each batch of HBSS is analyzed to determine if it contains any traces of bacteria or fungi. HBSS solution is available in gamma-irradiated PETG or PETE bottles. HBSS should be stored at 2-8°C and out of direct sunlight. Sterile procedures should be used for handling and regeneration of HBSS. Medically speaking, there are many requirements for artificial bones, dentures, or implants. In particular, the properties of this material are strictly required to have good biocompatibility, high specific strength and high fracture toughness, lightweight, small size, and other properties. Since magnesium is an essential element, magnesium implants can be an ideal biomaterial. Magnesium has a very low resistance to corrosion. No investigation of magnesium corrosion resistance in vivo or in vitro, Takaya reported the possibility of high pure magnesium to have good corrosion resistance in vitro. In this study, we focus explicitly on the behavior of magnesium alloys with HBSS solution under laboratory conditions [71]. I have used HBSS in immersion testing and potentiodynamic tests. Figure 3.2. shows the bottles that I used in some experiments.

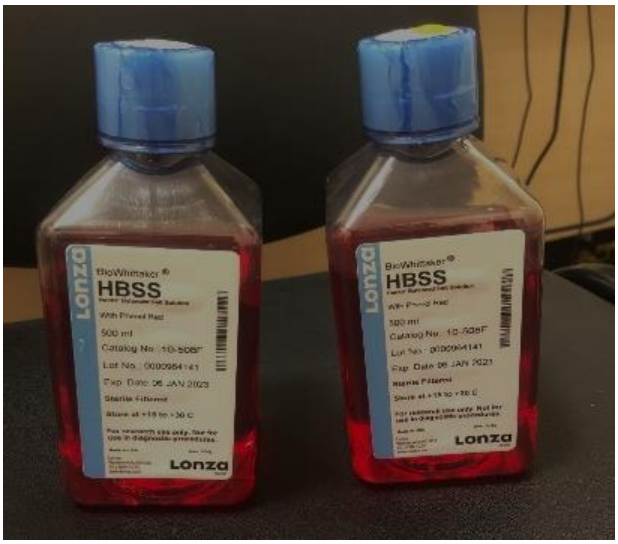

Figure 3.2. Hank's balanced salt solution (HBSS).

3.3. HOT ROLLING

After the material casting process, we get the AT31 alloy with dimensions (120 * 36 * 12) and it is entered for homogeneous heat treatment at a temperature of 400 ° C for 24 hours. After that, the alloy is kept in the sand to prevent it from oxidizing and distributing its heat during the homogenization process. After the homogenization process is completed, the ingot is entered into the hot rolling device to be hot rolled according to the information mentioned in Table 3.4. which shows the criteria by which the hot rolling was carried out, in addition to the narrowing of the section on the ingot by 20%, the total number of times (8) for each pass. After narrowing the section, we get 9 samples of AT31 alloy. The samples are mentioned in Table 3.5. which shows the speed applied to each sample.

Table 3.4. Rolling parameters.

Rolling temperature (°C)	Amount of section shrinkage per pass (%)	Rolling speed (m/min)	Total number of passes	Total section narrowing (%)	Initial and final thickness (mm)
400	20	1.5	8	~83	12-2
		4.7			
		10			

Table 3.5. Abbreviations for rolled specimen.

Rolling Speed	A	B	C
1.5 m/min	A1	B1	C1
4.7 m/min	A2	B2	C2
10 m/min	A3	B3	C3

3.4. IMMERSION TEST

Immersion tests determine how far a material will progress into the corrosion process based on the length of time it has been exposed to a corrosive environment, as well as the influence of other factors that can accelerate the corrosion process. In some cases, such as periodic testing, these tests may include alternating periods of drying and immersion. Furthermore, test instruments, such as connectors for electrochemical devices, can be inserted during the immersion process to facilitate measurements. Immersion tests are used in fields subject to immersion conditions because they are able to produce standardized alloy corrosion data. Industries that are fully involved in their own circumstances. The types of laboratory tests that should be performed are usually determined by the environmental conditions to be mimicked and the level of acceleration required. The following factors help in obtaining the desired acceleration. Extending the time an alloy is subjected to critical conditions perceived to cause corrosion damage. For example, if the vessel is to be treated with a chemical in batches for 24 hours, the recommended time for exposure to corrosion in the laboratory is 120 hours. Increasing the severity of the conditions to obtain a greater corrosion rate can be done by increasing the temperature, the salt concentration in the solution, pressure, or all four parameters at the same time [72]. After environmental factors have been identified and the test developed, the procedure needs to be repeated several times to determine whether the test meets the requirements for an acceptable degree of repeatability. In general, immersion tests can be classified into three categories. The periodic procedure, which involves immersing a sample for a specified period of time, is an alternative method of performing an immersion test. Next, the sample is removed

from the water and dried before being reintroduced into the cycle. Typically, approximately one hundred cycles are performed over the course of the test. A simple immersion test is the introduction of small samples of a substance into the medium being evaluated while noting the amount of weight lost over a certain period of time. In terms of examination methods, the immersion test remains the most reliable. It is also the easiest and most cost-effective means of evaluating the most appropriate materials to provide the greatest corrosion protection in certain scenarios [73].

During the immersion test experiment in the lab, I prepared and weighed all the samples separately. Then I recorded the weights before immersion in the solution and denoted them with the symbol (W-0). Then I immersed them in Hank's Balanced Salt Solution (HBSS) for 120 hours at a constant 37°C as shown in Figure 3.3. However, after 24 hours, I took the samples and cleaned them with an alcohol solution to remove Hank's Balanced Salt Solutions (HBSS) I dried them with a hair dryer for 2-5 minutes. After drying the samples well, I weighed all samples separately and recorded the weight after the first 24 h as (W-1). I did the same process every 24 hours until the 120 hours were up, so I got (W-2), (W-3), (W-4), and (W-5). We can see the weight recorded by each sample in Table 4.1.

Figure 3.3. Immersion test for all samples.

3.5. POTENTIODYNAMIC CORROSION TESTING

Electrochemical procedures, both quick and inexpensive, can be used to determine the electrochemical properties of a material. These methods rely in part on the ability to detect metallic corrosion by observing the response of the charge transfer process when subjected to electrochemical disturbance under controlled conditions. Corrosion of metallic implants within the human environment may have significant implications for biocompatibility and the safety of materials, making them a serious concern. The main component that corrodes the implant after its introduction into the body is the dissolution of the surface oxide, which leads to an increased release of metal ions. This results in unfavorable biological reactions that can be detected locally but may have systemic repercussions, ultimately leading to premature implant failure [74]. Polarization scanning obtained by force dynamism can be used to make predictions about the corrosion properties of the test sample. The use of polarization scanning allows extrapolation of the kinetic and corrosion properties of a metallic substrate. Charge transfer and the movement of reactants and products may slow or reduce the oxidation of electroactive species during the assay. Since polarization scanning is the only component that takes into account all these other factors, having a system that delivers reliable and reproducible scanning of polarization over several cycles is critical. The detection of these electrochemical parameters determines the corrosion factors of the material. A reliable and well-functioning wear system is required to achieve this. Sample erosion was achieved by the dynamic active polarization technique using a three-electrode configuration, consisting of reference, counter, and working electrodes. Before starting, a potential baseline is obtained. After stabilization of the corrosion potential (Ecorr), the applied potential is increased at a slow rate in the positive direction relative to the reference electrode [75].

During the potentiodynamic corrosion test experiment, I conducted in the laboratory, I prepared nine samples of AT31 Mg alloy with a surface area of 1 cm or less, which were hot-rolled differently. Next, I brought a copper wire to each sample and used double-sided tape to attach the wires to the samples themselves. Next, I placed each one inside a separate square-shaped plastic mold. In addition, I poured the resins into the molds and then left them until the resins hardened. Next, I grind the dried resin

from the bottom to remove the extra resin covering the sample. This is done so I can see the sample below. As shown in Figure 3.4. After I completed the grinding procedure, each sample was placed into a beaker that was heated to 37 °C and contained Hank balanced salt solution (HBSS). In addition, I attached cables coming from the computer to the wires connected to the samples, the reference electrode, and the auxiliary electrode. In the end, I started the potentiodynamic test, after which the results were displayed on the computer by the Gamry tool framework software. Figure 3.5. shows the last step of potential dynamic corrosion.

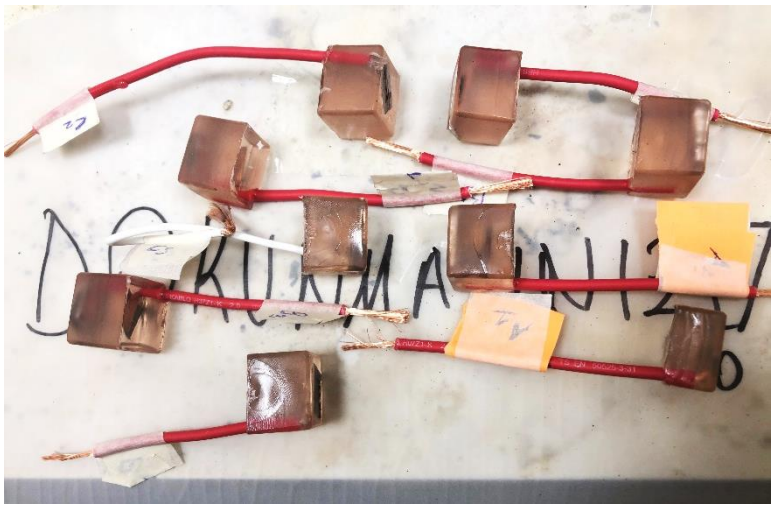

Figure 3.4. All samples after molding and grinding.

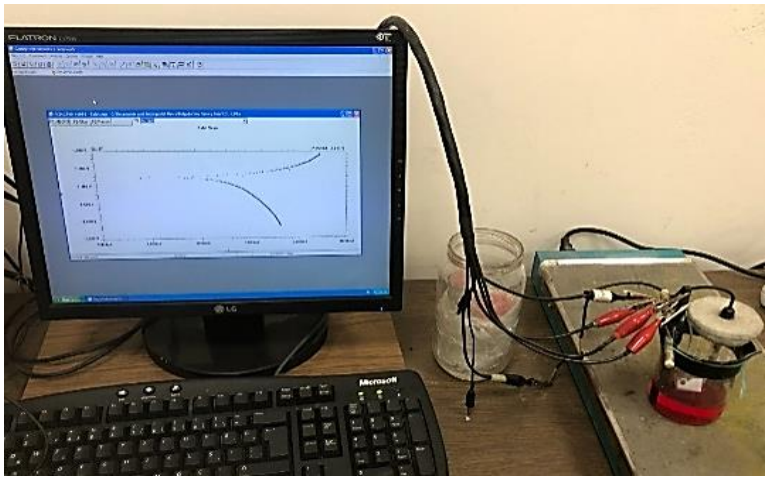

Figure 3.5. Potentiodynamic test with the Gamry tool framework software.

3.6. MICROSTRUCTURAL EXAMINATIONS

3.6.1. Sample Preparation

Acetic-picrate (10 ml distilled water, 5 gr picric acid, 70ml ethanol, and 5ml acetic acid) dispersant was prepared for post-roll microstructure investigations of the produced alloys. Before the corrosion tests, sanding with 2500, 1200, 800, and 600 sandpaper and polishing with 1µm felt were carried out and 1µm diamond suspension.

3.6.2. Optical Microscope and Scanning Electron Microscope Images

Using visible light and a series of lenses, an optical microscope magnifies images of microscopic materials. The optical microscope is the oldest type of microscope, and its current compound form was probably created in the 17th century. Optical microscopes use light instead of electrons to analyze objects. There are many designs of complex optical microscopes that aim to improve resolution and sample contrast, despite the relative simplicity of standard optical microscopes. Historically, optical microscopes were used because they use visible light, allowing samples to be seen with the naked eye and simplifying their development [76].

Using a focused electron beam, scanning electron microscopy (SEM) in Figure 3.6. is a powerful investigative method that creates comprehensive, high-magnification images of sample surface topography. After discovering and evaluating the region of interest in the sample using SEM, our experts will be able to delve deeper into the intricacies of the material using energy-dispersive X-ray spectroscopy (EDS) or energy-dispersive X-ray spectroscopy (EDX). They will be able to explore the content more carefully using these methods. SEM analysis, also known as scanning electron microscopy, provides high-resolution imaging that can be used to inspect a variety of materials for surface cracks, defects, inclusions, and corrosion. Our metallurgical experts apply SEM and EDX analysis to accurately analyze material properties and provide vital data to manufacturers. Examination of the optical surface with an electron microscope facilitates the detection of impurities or unknown particles, causes of failure, and material interactions. In addition to surface analysis, SEM can be used to

characterize particles, such as corrosion residues generated during testing. This is performed along with surface analysis. High magnification and high-resolution images allow SEM analysis to assess the number, size, and shape of small particles, allowing customers to understand the corrosion properties of their materials [77]. Homogeneous, microstructure, casting condition after rolling off the produced alloy examined by SEM, and Nikon Eclipse MA200 optical microscope in a laboratory Iron and Steel Institute of Karabuk University (KBÜ). Carl Zeiss Ultra Plus Gemini Fesem Scanning Electron Model.

Figure 3.6. Scanning electron microscope used for microstructure investigation.

PART 4

RESULTS AND DISCUSSIONS

4.1. X-RAY DIFFRACTION (XRD) ANALYSIS

The Ultima IV XRD instrumentation at the KBU Iron and Steel Laboratory XRD-XRF was used to determine the phases and texture of the alloys produced. XRD drawings were captured with a copper XRD instrument in the 15-90° range. From the XRD test on the AT31 magnesium alloy shown in the Figure 4.1. we can notice that all the peaks form the Mg phase and only one peak is depicted in a circle within the graph corresponding to the $Mg_{17}Al_{12}$ phase and the intensity of the peak increases with the increase of the Al content with reference to previous studies [78]. The $Mg_{17}Al_{12}$ phase was formed due to the stable phase with low temperature. In addition, when the proportions of the RE elements increase, new types of secondary phases, Al_2Gd, and Al-Mn are formed, and their peaks increase with the increase in the proportions of the RE elements, and with their increase, the $Mg_{17}Al_{12}$ phase is eliminated [79].

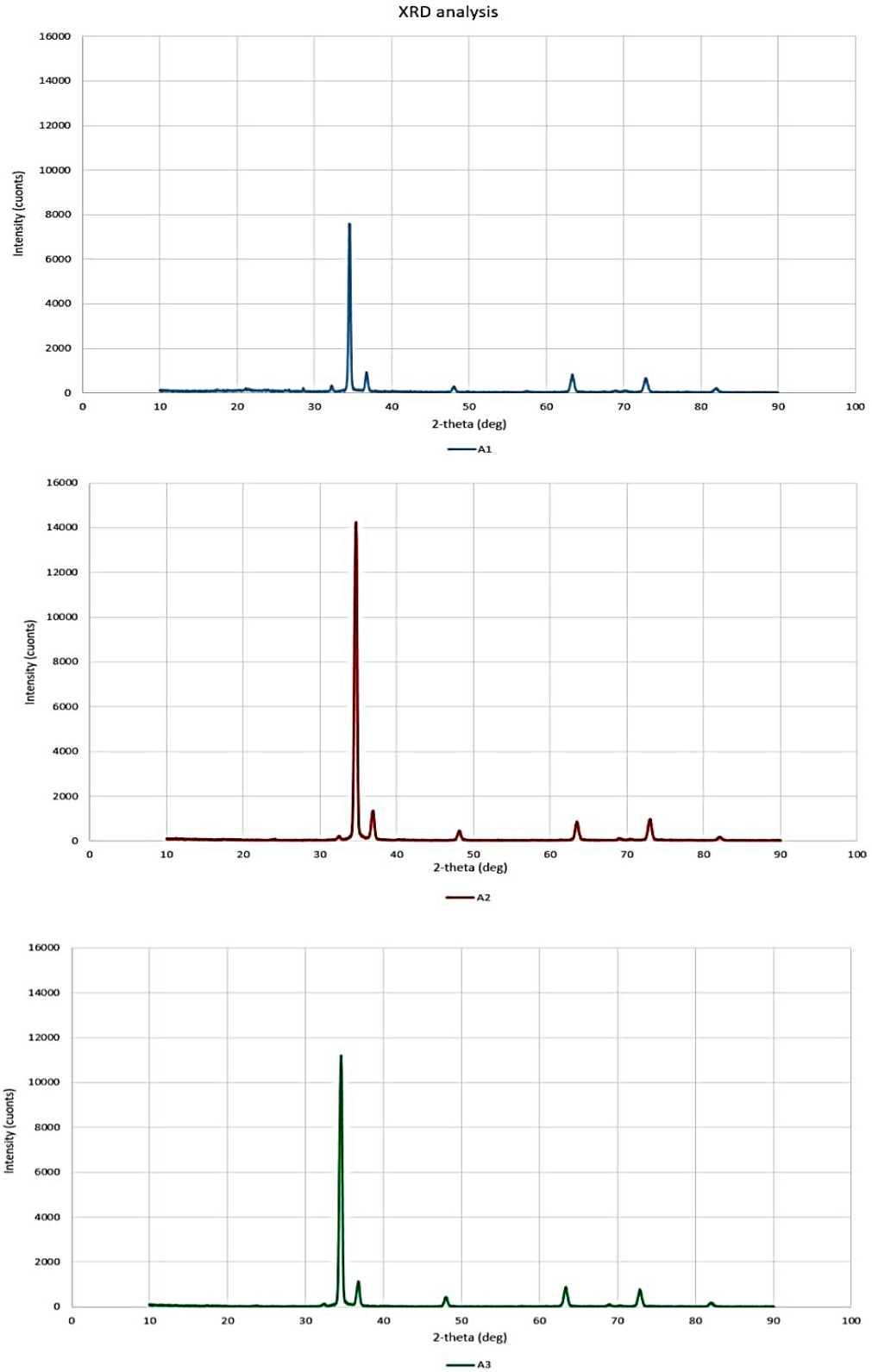

Figure 4.1. XRD Analysis of AT31 Mg alloy.

4.2. IMMERSION TEST

Samples were weighed and immersed in brine (HBSS) for five days (120 hours) in the laboratory of the Faculty of Engineering of Karabuk University, taken out, weighed, and then returned to solution every 24 hours for corrosion analysis and the reaction occurring in the magnesium alloy (AT31). During testing, we observed a gradual decrease in the weight of the samples, which indicates that the samples corrode due to their interaction with a salt solution at a constant temperature of 37 °C. The collected results can be found in Table 4.1. Figures 4.2, 4.3, and 4.4. listed below, show the results of the immersion process by the rate of sample weight loss during the immersion phase for all samples. Thus, we can say that the corrosion rate increases gradually as a result of the deposition of corrosion products during the immersion process in the initial stages [80]. In Figure 4.2. AT31 alloy (A1, A2, A3) was subjected to 20% deformation for each pass at different speeds of 1.5 m/min, 4.7 m/min, and 10 m/min, we note that it is A3 alloy at 10 m/min lost less weight than A2 and A1 at 4.7 and 1.5. We note that rolling speed has a clear effect on the samples in terms of grain diffusion, sample microstructure, and secondary phases. In addition, we observed the corrosion rate of sample A1 after 72 hours of immersion recorded with a negative value due to the increase in the weight of the sample compared to its original weight as shown in Table 4.1. It could indicate that the number of corrosion products deposited on the sample surface was very large [80].

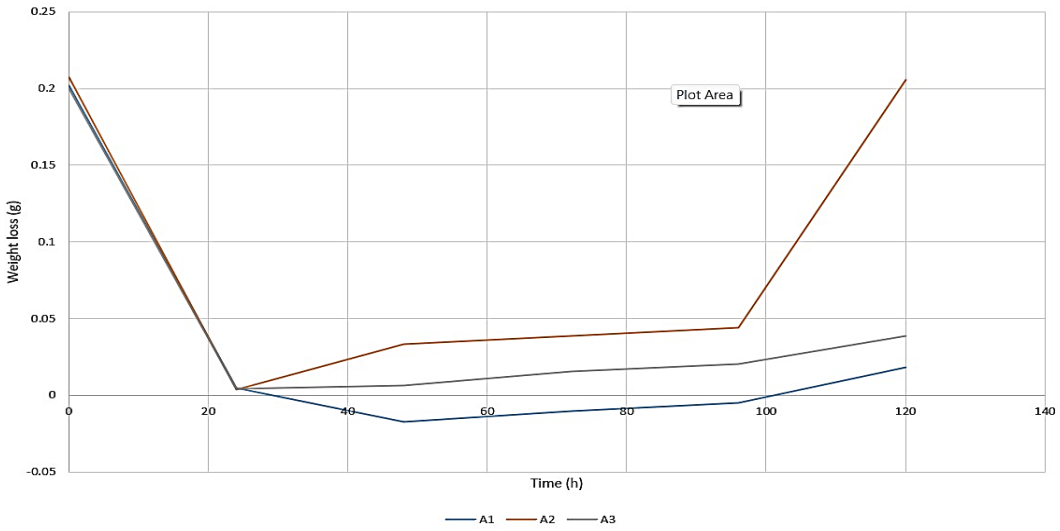

Figure 4.2. Chart of weight loss for A1, A2, and A3.

As shown in Figure 4.3. the best weight loss rate was for sample B1 which was subjected to 20% deformation for each pass, and the sample was rolled at a speed of 1.5 m/min compared to B samples, and the worst corrosion rate was for sample B3 that at rolled a speed of 10 m/min., it can be indicated that the size of fine particles and secondary phases in sample B1 is better than that of samples rolled at a higher speed.

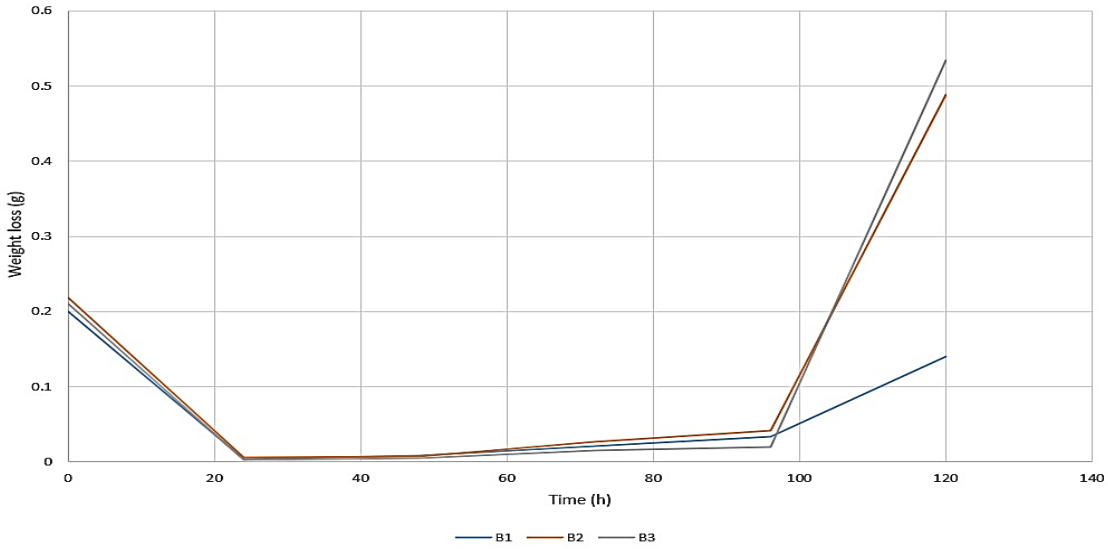

Figure 4.3. Chart of weight loss for B1, B2, and B3.

Figure 4.4. shows the weight loss of the AT31-C at different rolling speeds of 1.5, 4.7, and 10 m / min. The rate of weight loss for all samples C is relatively close because the proportions of RE elements that make up the sample are in the highest proportions compared to samples A and B. When comparing total weight loss, 4.7 m/min is the highest but 1.5 m/min is the lowest. The immersion test results for the corrosion rate of all rolled samples at rolling speeds of 1.5 m/min, 4.7 m/min, and 10 m/min with 20% deformation per lane are shown in Table 4.2.

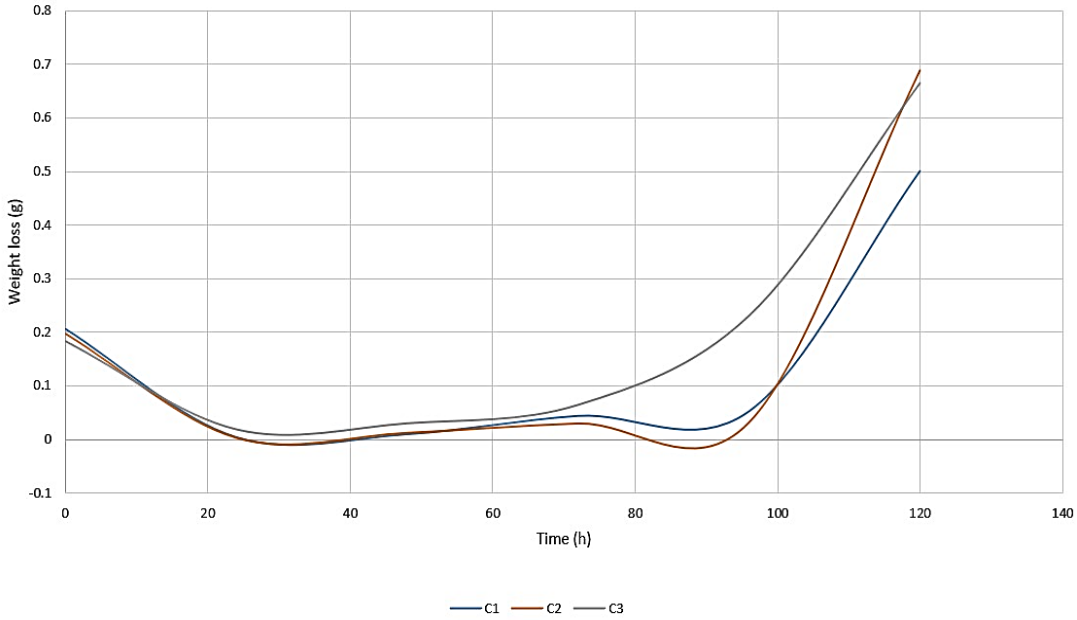

Figure 4.4. Chart of weight loss for C1, C2, and C3.

Table 4.1. Wight loss for each measurement duration.

Weight / Samples	W-0 (g)	W-1 (g)	W-2 (g)	W-3 (g)	W-4 (g)	W-5 (g)
A1	0.2019	0.2009	0.2054	0.204	0.2029	0.1982
A2	0.2075	0.2067	0.2006	0.1994	0.1983	0.1648
A3	0.2000	0.1991	0.1987	0.1969	0.1958	0.1922
B1	0.2004	0.1996	0.1988	0.1961	0.1936	0.1722
B2	0.2177	0.2164	0.2160	0.2118	0.2087	0.1112
B3	0.2096	0.2089	0.2084	0.2063	0.2055	0.0974
C1	0.2062	0.2054	0.2042	0.1971	0.1954	0.1027
C2	0.1978	0.1970	0.1952	0.1917	0.1913	0.0615
C3	0.1835	0.1801	0.1780	0.1716	0.1411	0.0613

From the previous Figures, we notice that the microstructure plays an important role in the rate of weight loss and corrosion for all samples of alloy AT31, where we notice that the rate of weight loss decreases directly with the decrease in the size of the grains

in the alloy [81]. The corrosion rate of magnesium alloys can be indicated through recent studies. the corrosion rate is affected by secondary phases in general. For example, the $Mg_{17}Al_{12}$ phase acts as a galvanic cathode that accelerates the corrosion process or acts as a block and delays the development of corrosion [82,83,84]. Magnesium alloy AT31 shows different secondary phase and grain sizes after the hot rolling process. The influence of rare elements on the size of the grains and secondary phases of the alloy must be considered, as the behavior of magnesium corrosion depends on the factors that have been mentioned [85,86]. The corrosion rate was calculated using Equation 4.1. and the corrosion results for all samples can be seen in Table 4.2. Through the results, we notice that the sample A3 rolled at a speed of 10m/min recorded the best corrosion resistance among all samples due to the fact that the grains are spread organized with their small size, which made them resist corrosion better. The coarse-grained region gets more powerful corrosion attacks than the fine-grained region, due to the higher disintegration density in the grainy regions, as happened in samples B AND C because they contain a high percentage of rare elements compared to samples A.

$$CR = (W0 - W \text{ after immersion}) (g) / \text{Area (mm)} * \text{Time (h)} \quad (4.1)$$

Table 4.2. Corrosion rate of immersion test with time.

Corrosion Rate	24h	48h	72h	96h	120h
A1	0.000309	-0.00226	-0.00202	-0.00128	0.005867
A2	0.000256	0.004417	0.007713	0.01169	0.068312
A3	0.000270	0.000820	0.003011	0.00535	0.012520
B1	0.000286	0.001196	0.004820	0.01011	0.052621
B2	0.000427	0.001124	0.005937	0.01210	0.179511
B3	0.000230	0.000804	0.003377	0.00561	0.193227
C1	0.000263	0.001293	0.008909	0.01420	0.170009
C2	0.000248	0.001760	0.006127	0.00871	0.230618
C3	0.001273	0.004117	0.013288	0.06348	0.228633

4.3. POTENTIODYNAMIC CORROSION TESTING

Looking at the dynamic effective corrosion curves of the AT31 and La-Gd group alloys in Figures 4.5,4.6, and 4.7. which are rolled at 1.5, 4.7, and 10 m/min rolling speeds with 20 percent deformation per pass. Clearly, Ecorr's value is closer to being positive. The data of Ecorr and Icorr of B1 with the rolled speed of 1.5 m/min and the ratio of 0.66 Gd was more deteriorated than other samples. On the other hand, the A3 sample with a rolled speed of 10 m/min and a ratio of 0.16 Gd has the greatest corrosion resistance. Corrosion resistance is happening for several reasons which are twinning percentage, recrystallized grains, variable textural strength, secondary phases with different shapes, distributing grain diameters, and solid-melt condition of the elements seen in the microstructure of Mg alloys after hot rolling which reduces in grain size. Some research that happened on corrosion resistance found grain size is an important reason for knowing how samples could resist. Other researchers show that grain boundaries are crystal flaws that reduce corrosion resistance [87]. On the other hand, other researchers show that grain boundaries are a barrier that increases corrosion resistance. Significant research has been conducted on how secondary phases impact corrosion resistance. The researchers compared the effects of grain size and secondary phases on corrosion resistance. Moreover, it has been stated that the corrosion resistance of the sample with the largest secondary phases and smallest grains is weak. However, massive secondary phases served as cathodes and inhibited the impact of tiny particles but when the secondary phases comprised the smallest proportion and the grains were quite coarse, the corrosion resistance was weak. Here, coarse grains had a predominating impact. In the research, samples with a medium secondary phase and an average grain size exhibited the best corrosion resistance [88]. According to Melnikov et al., the Al-Mn secondary phases operate a galvanic cathode in accordance with the Mg matrix, and these particles are the origins of galvanic corrosion. They stated that growing Al-Mn secondary phases had a negative impact on the material's corrosion resistance [89]. Examining the secondary phase distributions and dimensions of the 20% deformation alloys reveals that, as the rolling speed increases, the secondary phases become thinner and more uniformly scattered in smaller intervals. At a rolling speed of up to 10 m/min, secondary phases accumulated at grain boundaries and decreased metal loss. This is consistent with the research [90].

A similar scenario held true for La-Gd alloys with a 20% deformation, and the corrosion rate of alloys with a rolling speed of 4.7 m/min, which exhibited a more frequent and homogenous distribution with increasing Gd content, was superior. In research, it was indicated that the broken lattice atoms that result from twinning with crystal defects increase corrosive assaults on the material [91]. From Figure 4.5. we notice that the values of sample A3 with a rolling speed of 10 m/min register the best rate value (0.0013) for the rest of the samples with lower speeds.

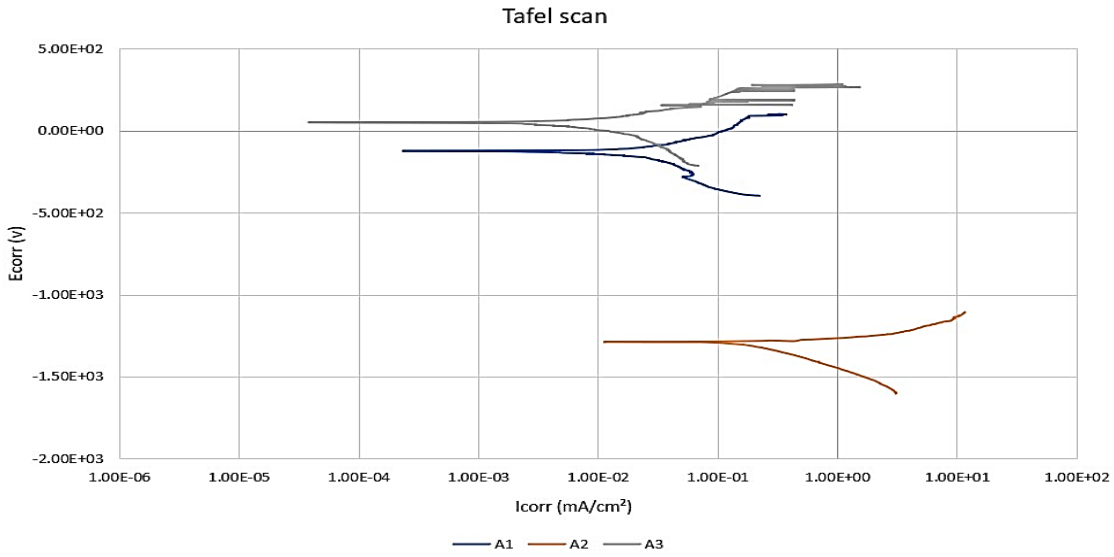

Figure 4.5. Potentiodynamic chart of Mg alloys AT31 (A1, A2 and, A3).

In the Figure 4.6. we notice in the diagram that B2 rolled at a speed of 4.7 m/min recorded the best rate values (0.3857) for B samples rolled at different speeds, and we also note the deterioration of the corrosion rate value for sample B1(0.5901) rolled at a speed of 1.5 m/min.

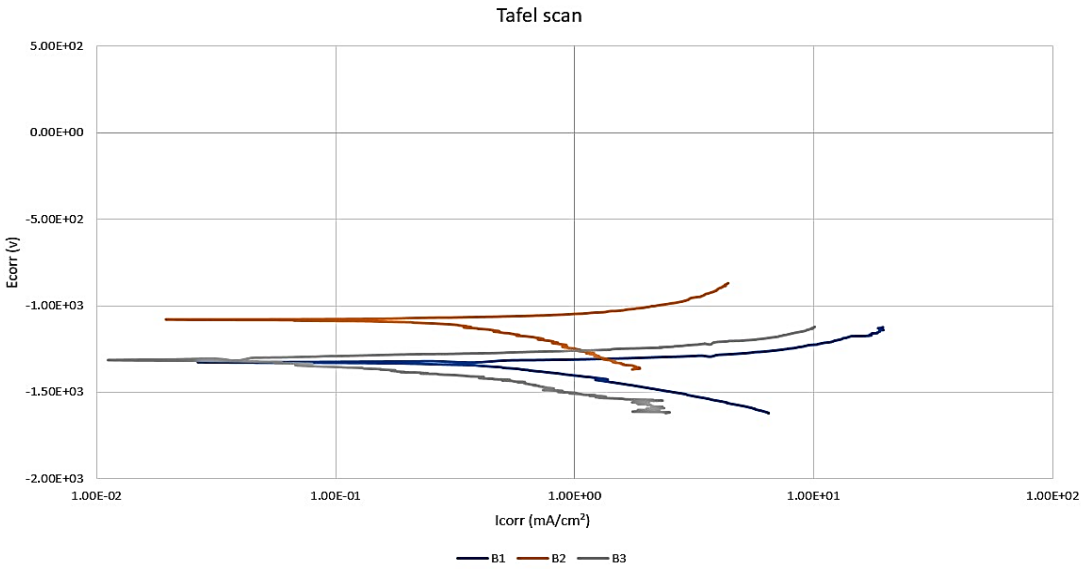

Figure 4.6. Potentiodynamic chart of Mg alloys AT31 (B1, B2 and, B3).

The best value of the corrosion rate was recorded as C1(0.0529) that rolled at speed 1.5 m/min for the rest of the C samples as shown in the Figure 4.7. In addition, the values of the corrosion rate in the C2 and C3 samples are very close.

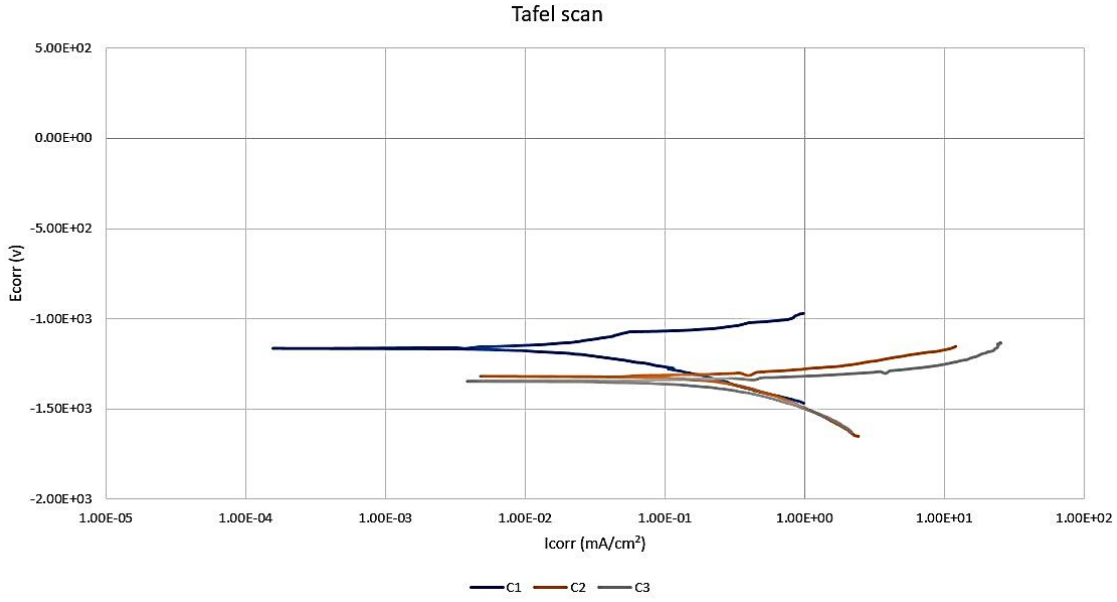

Figure 4.7. Potentiodynamic chart of Mg alloys AT31 (C1, C2, and C3).

From the previous diagrams, results, and research it was observed that the best values of resistance corrosion recorded for all samples are A3 that rolled at a speed of 10 m/min, with a small percentage of RE elements compared to samples B and C. The

best resistance values for samples C are C1, which has higher proportions of elements in the alloy than samples A, and B, but with a rolling speed of 1.5 m/min. Corrosion resistance is increased by decreasing the values of RE elements percentage included in the alloy composition and by increasing the rolling speed to obtain an improvement in corrosion state. The increase in the percentage of RE elements leads to the formation of coarse grain size that contributes to the deterioration of the alloy when exposed to the salt solution. Rolling speed has an important influence on the alloy in terms of microstructure, grain diffusion, rolling direction, and formation of atomic boundaries. The corrosion rate for all samples was recorded in Table 4.3.

Table 4.3. Result of corrosion rate by potentiodynamic test.

Samples	Ecorr (v)	Icorr (mA/cm²)	Corrosion rate (mpy)
A1	-0.121	0.0176	0.0216
A2	-1.290	0.210	0.2578
A3	0.053	0.00114	0.0013
B1	-1.330	0.488	0.5901
B2	-1.080	0.319	0.3857
B3	-1.310	0.0675	0.0816
C1	-1.160	0.0447	0.0529
C2	-1.320	0.248	0.2937
C3	-1.350	0.246	0.2913

4.4. MICROSTRUCTURAL EXAMINATIONS

4.4.1. Optical Microscope Images

In Figure 4.8. optical micrographs of the alloys are shown AT31 alloy's as-cast microstructure consists of -Mg matrix and separated eutectic -$Mg_{17}Al_{12}$ phases, however, there is a modest drop in grain size in the A1 sample owing to an increase in Al content. This is due to the fact that when Al content rose, grain size reduced It was revealed that grain size dropped considerably across all samples. The findings support the idea that an increase in the Gd/Al ratio induces a detectable increase in grain size. This corroborates the findings of more recent research on aluminum and magnesium alloys, which demonstrate higher grain-refining capabilities compared to alloys of the

same kind refined using rare earth elements [92]. Due to the influence of grain growth restriction, it was emphasized that the most important aspect of grain refining is an increase in the volume fraction of the secondary phase. This was reinforced several times. The most critical components were the inclusion of aluminum, which induced aluminum enrichment throughout the solidification process, and constitutional undercooling in a diffusion layer right before the solid/liquid interface. Even today, there is a range of morphological variations of the main grain. In addition, as Gd and Al content increases, the distribution of secondary phases penetrates interdimeric regions and presents a coarse and uniform network [93].

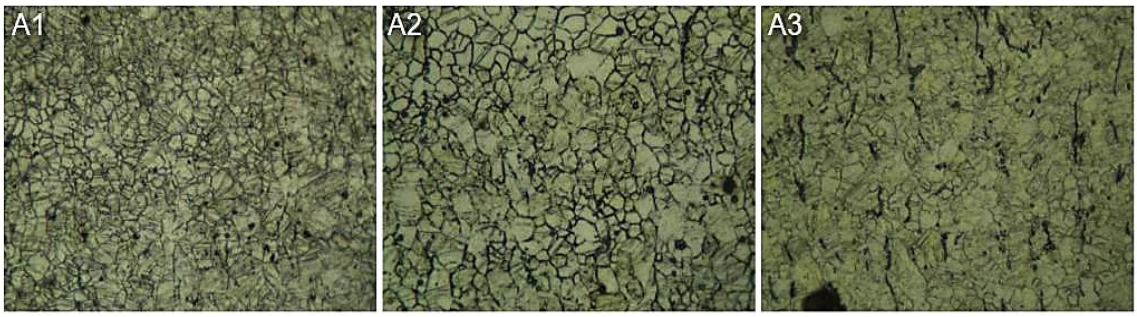

Figure 4.8. Optical microscope images of specimen A1, A2, and A3.

In Figure 4.8. optical microscope images are given after rolling the AT31 alloy at 20% deformation rate and at rolling speeds of 1.5 m/min, 4.7 m/min and 10 m/min.

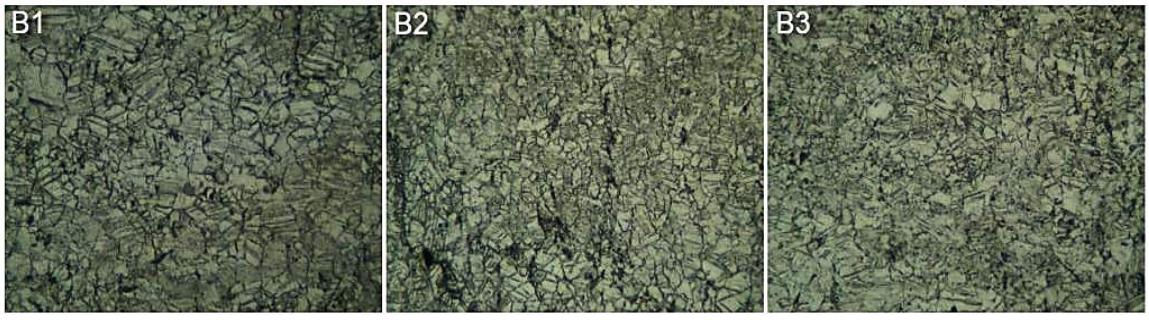

Figure 4.9. Optical microscope images of specimen B1, B2, and B3.

In figure 4.9. twinning occurred in the grains of AT31 Mg alloy, which underwent 20% deformation per pass at rolling speeds of 1.5 m/min, 4.7 m/min, and 10 m/min.

However, the AT31 Mg alloy, which underwent 20% deformation at a rolling speed of 4.7 m/min and 10 m/min, had more recrystallized grains.

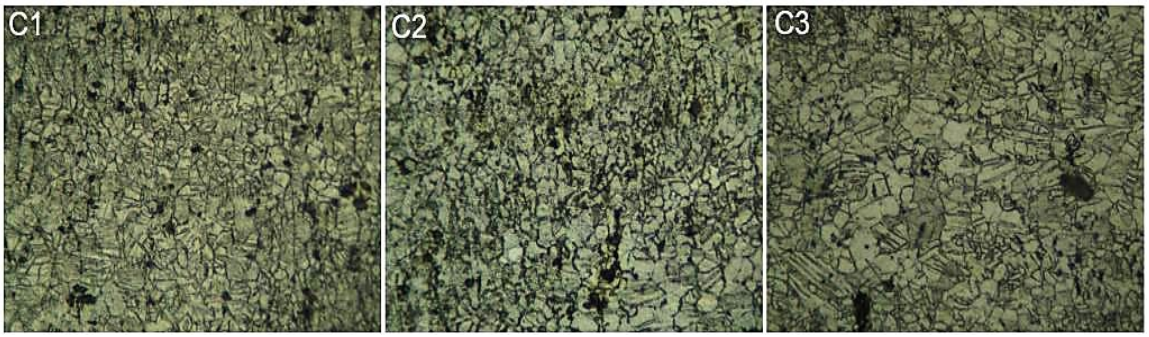

Figure 4.10. Optical microscope images of specimen C1, C2, and C3.

In Fig. 4.10. the optical images of AT31 Mg alloy show some fine grain, twin, and coarse-grained with the addition of 1.33% Gd, which underwent 20% deformation per track at 1.5 m/min, 4.7 m/min, and 10 m/min rolling speed. However, the recrystallized grains can be detected from the optical microscopy images. In addition, it is noticeable that the deformed samples with 20% per track and high percentages of RE elements have coarse grains with increasing winding speed.

4.4.2. Scanning Electron Microscope Before Corrosion Test

Figure 4.11. shows enlarged SEM images drawing secondary phases of the AT31 alloy before the corrosion tests. According to the results of EDS and XRD patterns, there are studies confirming that the continuous network marked by arrow A at the boundary is $M_{17}Al_{12}$. It is observed that there is an increase in the distribution of the second phase due to the increase in the amount of aluminum deposited, especially in the sample containing 2.5% by weight Al, and the secondary phases are very dense. It was also determined that these secondary phase sediments were irregularly dispersed at the grain boundaries and within the grains. Tang et al studied the secondary phase on magnesium alloys using magnesium alloy AZ33 and found that the secondary phases were distributed along the grain boundaries as a continuous or semi-continuous network [94].

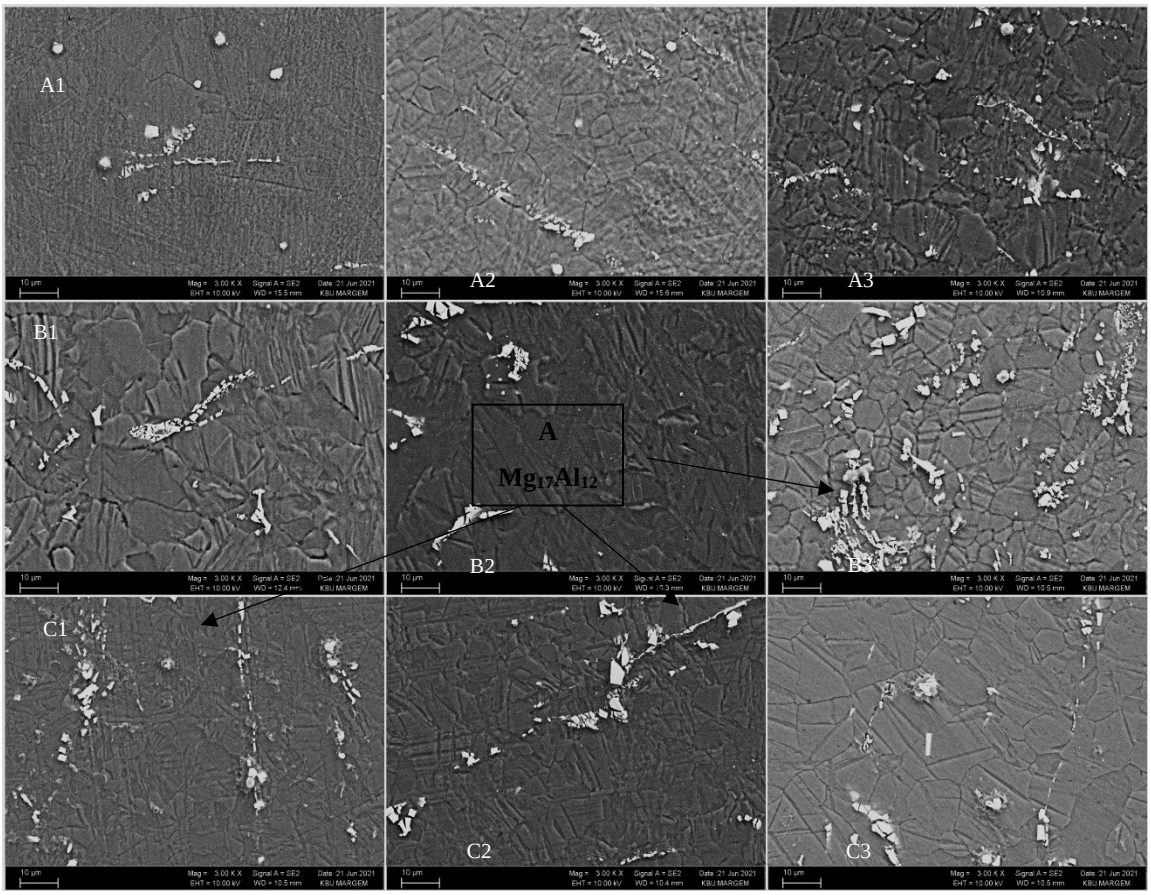

Figure 4.11. (SEM) images of rolled materials A1, A2, A3, B1, B2, B3, C1, C2, and C3.

As can be seen in the Figures 4.11. widely dispersed polygonal and spherical secondary phases were for in AT31 Mg alloys, which underwent 20% deformation per pass at a rolling speed of 1.5 m/min 4.7 m/min, and 10 m/min. In addition, there are larger spherical-shaped secondary phases at a rolling speed of 10 m/min than at a rolling speed of 4.7 m/min. However, AT31 Mg alloys, which underwent 20% deformation at rolling speeds of 4.7 m/min and 10 m/min, widely dispersed thin spherical shaped secondary phases formed in a certain area, respectively. Here, it is seen that with increasing rolling speed, the secondary solutions line up along the grain boundaries and dissolve in the matrix.

4.4.3. Scanning Electron Microscope After Corrosion Test

Figure 4.12. shows the scanning electron microscopy (SEM) analysis of the surface of AT31 alloy after corrosion tests which are the potentiodynamic test and the immersion

test (120 hours of immersion in HBSS containing Mg^{2}+ and Ca^{2}+ ions). The microstructure of AT31 alloy consists of an alpha matrix and a few additional types of metallic components. More specifically, if phase $Mg_{17}Al_{12}$ is present [95]. The volume ratio of the $Mg_{17}Al_{12}$ phase has been shown to influence the rate of dissolution by acting either as an anodic barrier or as a galvanic cathode in many magnesium alloys. This discovery is made possible because $Mg_{17}Al_{12}$ can operate in both capacities. After immersion in the solution for five days, the corrosion layers that arose on the surfaces of AT31 were uniform in shape and texture see Fig. 4.12. For example, in both alloys dipped in Hanks' solution, the CP layers were less uniform and some cracks appeared. Attacks look smooth. However, the CP layers are very broken. On the surface of AT31, there are still a few gray spots corresponding to the phase $Mg_{17}Al_{12}$ and some white particles bound to the interfacial Al-Mn metals [96]. It can be said that these areas act as local cathodes.

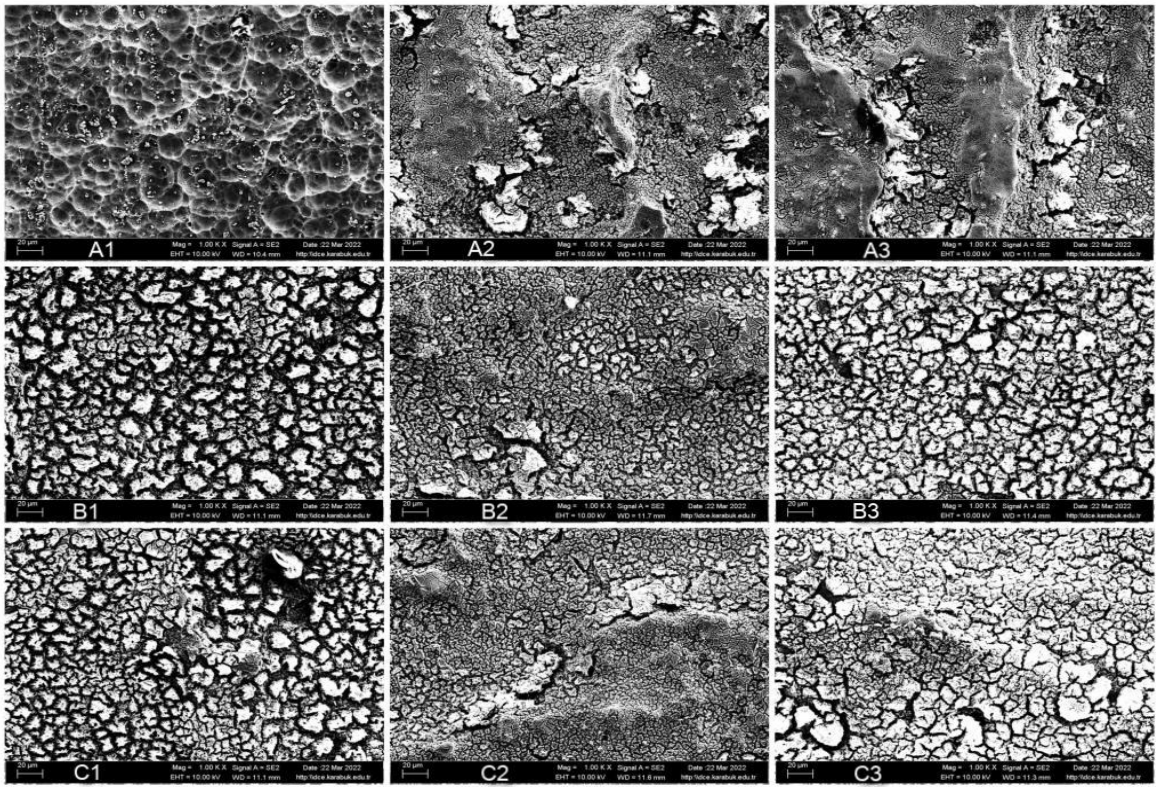

Figure 4.12. SEM images of rolled materials after corrosion A1, A2, A3, B1, B2, B3, C1, C2, and C3.

4.4.4. Energy Dispersive Spectroscopy (EDS)

Figure 4.13. shows an SEM micrograph of the sites examined by EDS. The following images show the results of the EDS study. In the secondary phase of $Mg_{17}Al_{12}$, EDS analysis indicates the establishment of an independent network. The presence of the Gd-containing components is indicated by both the rod-shaped phases and the small, block-shaped phases. When the Gd content of a substance exceeds 0.5 wt.%, a new mass-shaped phase begins in the microstructure, it seems that the addition of Gd greatly affects the alloy as metallic phases and the Al_2Gd phase is formed at the expense of the $Mg_{17}Al_{12}$ phase [97]. The EDS findings indicate that Al and Gd may be identified at this location. Based on the XRD pattern and the almost 2:1 molar ratio of Al to RE (Gd and Nd), this block-shaped phase may be classified as the Al_2Gd phase. In addition, the size and quantity of Al_2RE phases increase directly with increasing Gd content. Previous research indicates that the Al_2RE phase is mostly composed of Gd and Y RE elements [98].

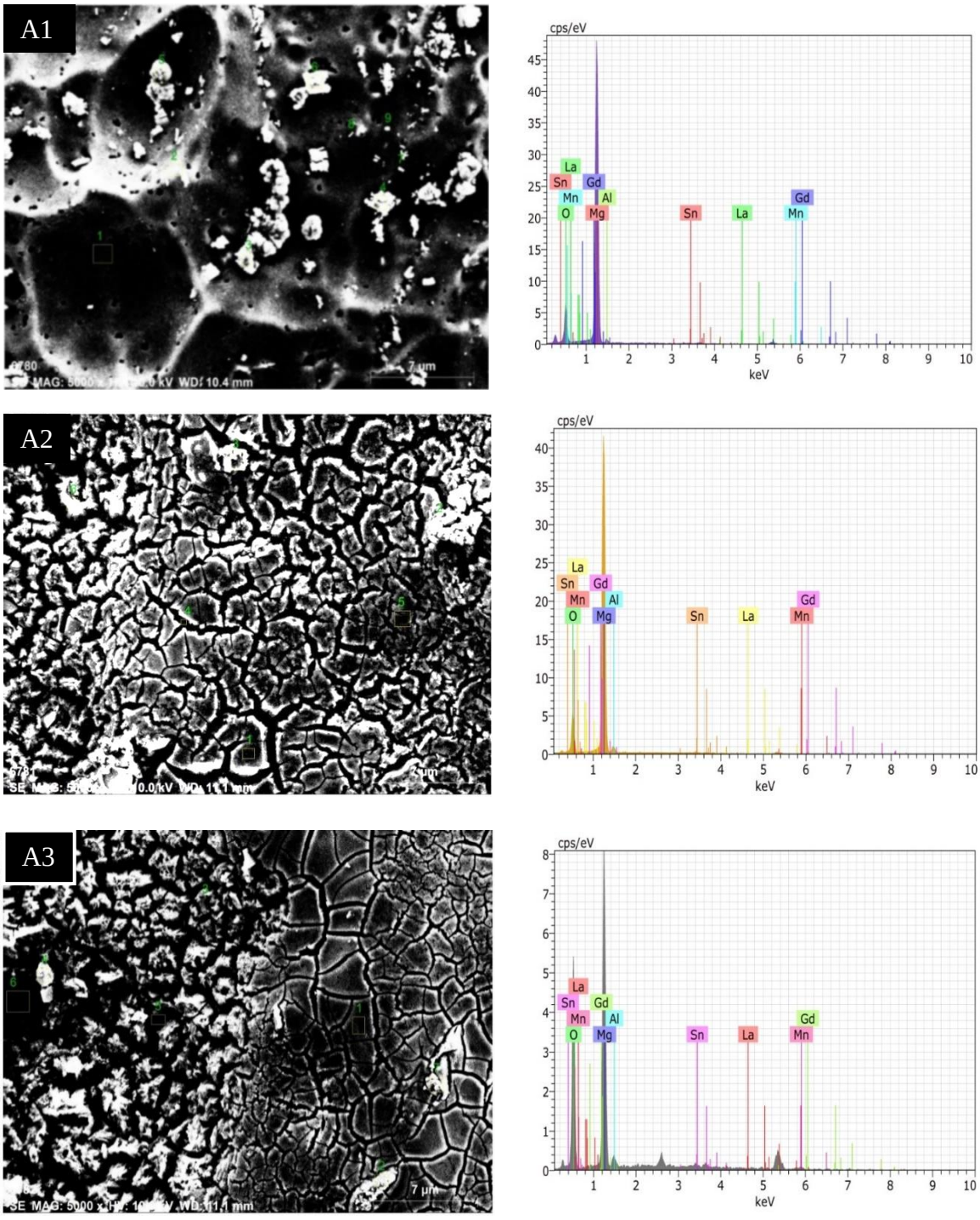

Figure 4.13. EDS analysis for all samples of Mg AT31 alloy.

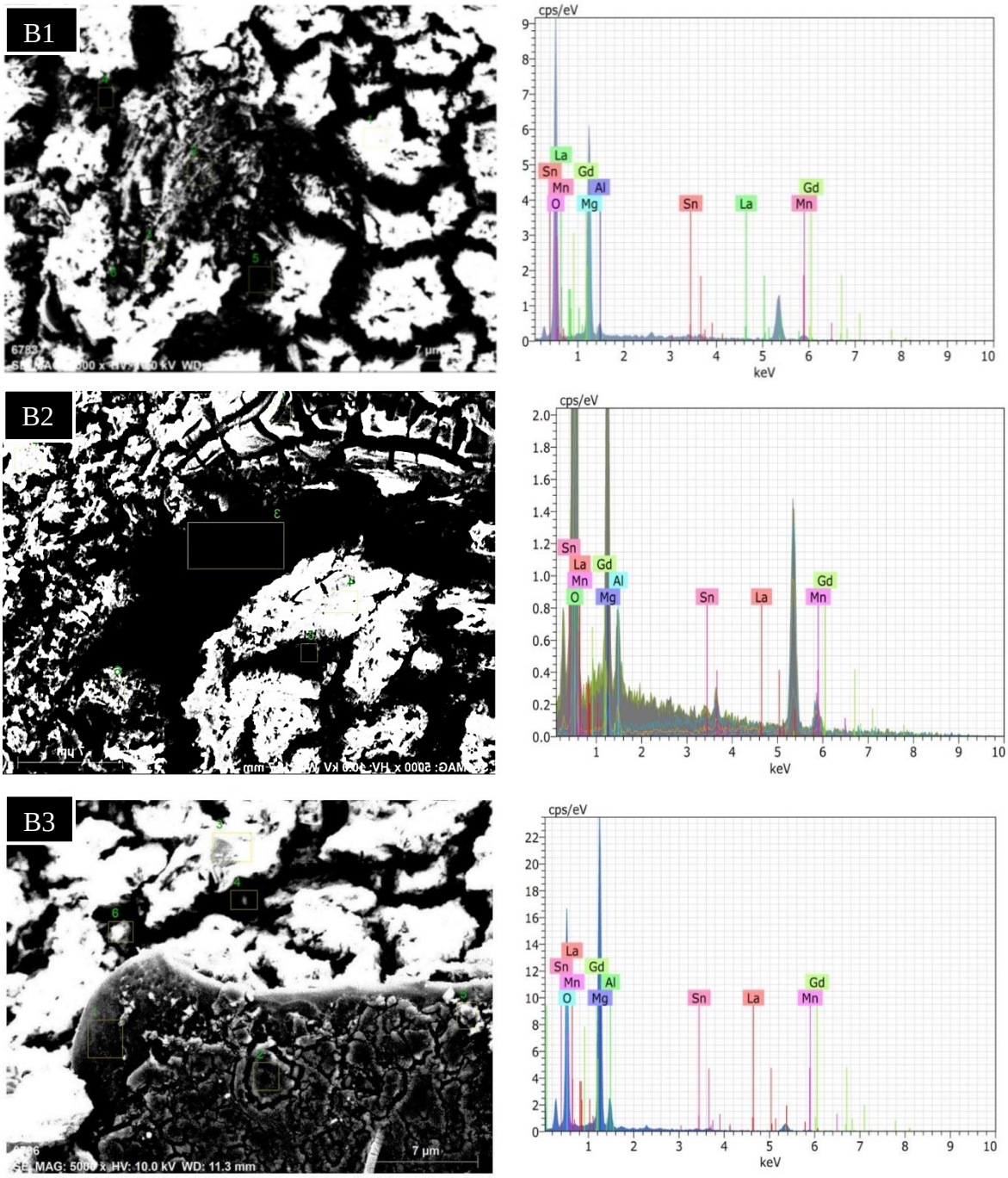

Figure 4.14. EDS analysis for all samples of Mg AT31 alloy.

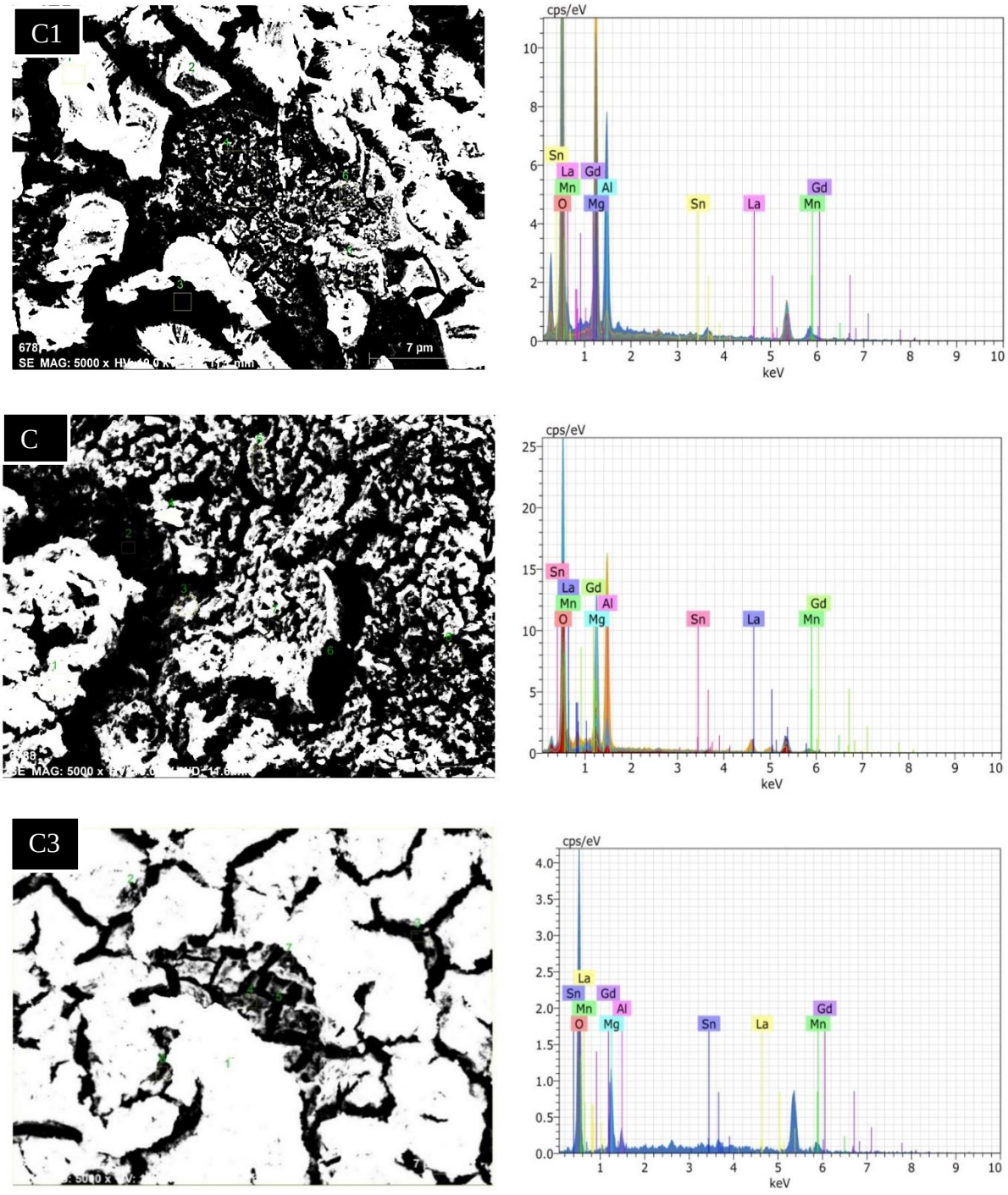

Figure 4.15. EDS analysis for all samples of Mg AT31 alloy.

CONCLUSIONS

- The hot rolling process included three different rolling speeds of 1.5, 4.7, and 10 m/min which changed the microstructure of the investigated samples of Mg-Al-Sn-La-(0.16,0.66, 1.33) Gd alloy. After examining the results of the immersion test in Hank's solution of the samples, it was noted that the best corrosion resistance was obtained in samples A1 (0.005867) and A3 (0.012520), and the worst was measured in C2 (0.230618). Also, it was noted that the best corrosion resistance of the samples was A3 (0.0013) and the worst (0.5901) by the potentiodynamic test. The different results were collected due to the different microstructural characteristics of the samples such as the formation of twins, average grain size, and the distribution of secondary phases on the matrix.
- Corrosion resistance is affected by two main factors, one is the grain size and the other is the secondary phases of the sample.
- It can be seen that the best values of corrosion resistance are those with high rolling speed. It can be said that the rolling speed effects on the grain size of the sample, increasing the speed leads to a decrease in the grain size.
- Through XRD examination, secondary phases that contribute to corrosion resistance are found, such as the Mg2Sn phase.

REFERENCES

1. Lu, Y., Bradshaw, A. R., Chiu, Y. L., & Jones, I. P. (2015). Effects of secondary phase and grain size on the corrosion of biodegradable Mg–Zn–Ca alloys. *Materials Science and Engineering: C*, *48*, 480-486.

2. Caldeira, J. P. E. (2011). *Estudo da resistência à corrosão de ligas de magnésio para a indústria automóvel* (Doctoral dissertation).
3. [3] Cao, F., Shi, Z., Song, G. L., Liu, M., Dargusch, M. S., & Atrens, A. (2015). Influence of hot rolling on the corrosion behavior of several Mg–X alloys. *Corrosion Science*, *90*, 176-191.

4. A.A. Luo, K. Sadayappan, Technology for Magnesium Castings, American Foundry Society, Schaumburg, IL, 2011, pp. 29–47.

5. W. J. Xia, Z. H. Chen, D. Chen, S. Q. Zhu, Microstructure and mechanical properties of AZ31 magnesium alloy sheets produced by differential speed rolling, Mater.Process, Technol, 209 (2009), 26–31, doi: 10.1016/j.jmatprotec.2008.01.045.

6. Hirsch, J., Skrotzki, B., & Gottstein, G. (Eds.). (2008). *Aluminium alloys: the physical and mechanical properties* (Vol. 1). John Wiley & Sons.

7. Proceedings of the International Symposium on Quality and Process Control in the Reduction and Casting of Aluminum and Other Light Metals Winnipeg, Canada, August 23-26, 1987, Vol. 5 Proceedings of the Metallurgical Society of the Canadian Institute of Mining and Metallurgy.

8. Mezbahul-Islam, M., Mostafa, M., & Medraj, M., "Essential Magnesium Alloys Binary Phase Diagrams and Their Thermochemical Data", Journal of Materials, (2014).

9. Baker, H., "Alloy Phase Diagrams". ASM Handbook, (Cilt 3) pp. 280-285 (1998).

10. Raynor, G.V.; Smith R.W. Proc. R. Soc. 1958, 244, 101-109.

11. Sundgren, J. E. (1985). Structure and properties of TiN coatings. *Thin solid films*, *128*(1-2), 21-44.

12. Ojima, K; Takasaki, A. Philos. Mag. Lett. 1993, 68(4), 237-244.

13. Porter, F. C. (1991). *Zinc handbook: properties, processing, and use in design*. Crc Press.

14. Lynch, R.F. Zinc: Alloying, Thermomechanical Processing, Properties, and Applications. In Encyclopedia of Materials: Science and Technology; Elsevier: Amsterdam, The Netherland, 2001; pp. 9869–9883.

15. Moezzi, A., McDonagh, A. M., & Cortie, M. B. (2012). Zinc oxide particles: Synthesis, properties and applications. *Chemical engineering journal*, *185*, 1-22.

16. Rollez, D.; Pola, A.; Prenger, F. Zinc alloy family for foundry purposes. World Metall. 2015, 68, 354–358.

17. Huerman Eric, R. "An overview on manganese alloy production and related fundamental research in South Africa." *Mineral Processing and Extractive Metallurgy Review* 15.1-4 (1995): 191-200.

18. Rao, C. N. R., & Raveau, B. (1998). *Colossal magnetoresistance, charge ordering and related properties of manganese oxides*. World Scientific.

19. Chao, C.Y., Liu, C.H., Materials Transactions, 43(10), 2635, 2002.

20. Mordike, Bl. (2002). Creep-resistant magnesium alloys. Materials Science and Engineering: A, 324(1), pp.103-112.

21. Dan'Kov, S. Y., Tishin, A. M., Pecharsky, V. K., & Gschneidner, K. A. (1998). Magnetic phase transitions and the magnetothermal properties of gadolinium. *Physical Review B*, *57*(6), 3478.

22. Zhu, Su-Ming., Gibson, Ma., Easton, Ma and Nie, Jf. (2010). The relationship between microstructure and creep resistance in die-cast magnesium–rare earth alloys. Scripta Materialia, 63(7), pp.698-703.

23. Weast, Robert (1984). CRC, Handbook of Chemistry and Physics. Boca Raton, Florida: Chemical Rubber Company Publishing. pp. E110. *ISBN 0-8493-0464-4*

24. C. Blawert, N. Hort, KV. Kainer, Automotive Applications of Magnesium and Its Alloys. Trans. Indian Inst. Met. Vol. 57, No. (4), 2004 , pp. 397–408

25. Tekumalla, S., Seetharaman, S., Almajid, A., & Gupta, M., "Mechanical Properties of Magnesium-Rare Earth Alloy Systems: A Review", Metals, 5: s. 1-39 (2014).

26. Hort, N., Huang, Y., Fechner, D., Störmer, M., Blawert, C., Wittle, F., Feyerabend, F., "Magnesium alloys as implant materials – Principles of property design for Mg– RE alloys", Acta Biomaterialia, 6(5): s. 1714-1725 (2010).

27. CHAKRABORTY, I. N., SHELBY, J. E., & CONDRATE, R. A. (1984). Properties and structure of lanthanum borate glasses. *Journal of the American Ceramic Society*, *67*(12), 782-785.

28. C Blawert, N. Hort, KV. Kainer, Automotive Applications of Magnesium and Its Alloys. Trans. Indian Inst. Met. Vol. 57, No. (4), 2004, pp. 397–408.

29. W. Qu- Dong and L. Yi -Zhen, Mater. Sci. Eng. Vol. A 278, 2000, p. 66

30. Homojenleştirme işlemiyle ince yapılı ikincil fazlar yapıda çözünmüş ve tane sınırları daha belirgin hale gelmiştir.

31. Luo, A., "Magnesium casting technology for structural applications", Journal of Magnesium and Alloys, 1: 2-22 (2013)

32. K.U. Kainer (Ed), Magnesium - Alloys and Technology, WILEY-VCH Verlag Gmbh & Co. KG aA, Weinheim 2003.

33. Avedesian, M. M., & Baker, H. (1999). ASM speciality handbook: magnesium and magnesium alloys. *ASM international*, *274*.

34. Gupta, M., & Ling, S. N. M. (2011). *Magnesium, magnesium alloys, and magnesium composites*. John Wiley & Sons.

35. ASTM Standard B 275 Standard Practice for Codification of Certain Nonferrous Metals and Alloys, Cast and Wrought.

36. Hermawan, H. (2012). Biodegradable metals: state of the art. *Biodegradable Metals*, 13-22.

37. Hermawan, H. (2012). *Biodegradable metals: from concept to applications*. Springer Science & Business Media.

38. L. Lopez, M.W. Carter, M. Gendreau, The hot strip mill production scheduling problem: A tabu search approach, European Journal of Operational Research, 106 (2-3) (1998), pp. 317-335

39. Colas, R., Ramırez, J., Sandoval, I., Morales, J. C., & Leduc, L. A. (1999). Damage in hot rolling work rolls. *Wear*, *230*(1), 56-60.

40. Dalland, O., & Nes, E. (1996). Origin of cube texture during hot rolling of commercial Al□ Mn□ Mg alloys. *Acta materialia*, *44*(4), 1389-1411.

41. Course, N. B. C. (1971). National Association of Corrosion Engineers. *Houston, Tex*, 9-2.

42. Postlethwaite, J., & Nešić, S. (2011). Erosion–Corrosion: Recognition and Control. Uhlig's Corrosion Handbook, 907-913.

43. Makar, G. L., & Kruger, J. L. (1993). Corrosion of magnesium. International materials reviews, 38(3), 138-153.

44. Singh, I. B., Singh, M., & Das, S. (2015). A comparative corrosion behavior of Mg, AZ31 and AZ91 alloys in 3.5% NaCl solution. Journal of Magnesium and Alloys, 3(2), 142-148.

45. Corrosion Doctors, 2008, http://corrosion-doctors.org/

46. Mao, L., Yuan, G., Wang, S., Niu, J., Wu, G., & Ding, W. (2012). A novel biodegradable Mg–Nd–Zn–Zr alloy with uniform corrosion behavior in artificial plasma. Materials Letters, 88, 1-4.

47. Clark, K. J. (1986). AZ 91 E Magnesium Sand Casting Alloy: the Standard for Excellent Corrosion Performance. In 43 rd Annual World Magnesium Conference, Proceedings (pp. 37-41).

48. Wei Guo, K. (2011). A review of magnesium/magnesium alloys corrosion. Recent Patents on Corrosion Science, 1(1), 72-90.

49. Avedesian, M. M., & Baker, H. (Eds.). (1999). ASM specialty handbook: magnesium and magnesium alloys. ASM international.

50. Murray, R. W., & Hillis, J. E. (1990). Magnesium finishing: chemical treatment and coating practices.

51. Hillis JE and Murray RW (1987) Finishing Alternatives for High Purity Magnesium Alloys, Paper G T87-, Society of Die Casting Engineers 14th International Congress and Exposition, Toronto.

52. Bundy, K. J. (1994). Corrosion and other electrochemical aspects of biomaterials. Critical Reviews in Biomedical Engineering, 22(3-4), 139-251.

53. Austin, S. A., Lyons, R., & Ing, M. J. (2004). Electrochemical behavior of steel-reinforced concrete during accelerated corrosion testing. Corrosion, 60(2), 203-212.

54. Clark, K. J. (1986). AZ 91 E Magnesium Sand Casting Alloy: the Standard for Excellent Corrosion Performance. In 43 rd Annual World Magnesium Conference, Proceedings (pp. 37-41).

55. Pinto, R., Carmezim, M. J., Ferreira, M. G. S., & Montemor, M. F. (2010). A two-step surface treatment, combining anodisation and silanisation, for improved corrosion protection of the Mg alloy WE54. Progress in Organic Coatings, 69(2), 143-149.

56. Tsukerman, S. A. (2013). Powder metallurgy. Elsevier.

57. Hu, H., Nie, X., & Ma, Y. (2014). Corrosion and surface treatment of magnesium alloys. Magnesium Alloys-Properties in Solid and Liquid States, 67-108.

58. Guo, K. W. (2010). A review of magnesium/magnesium alloys corrosion and its protection. Recent Patents on Corrosion Science.

59. Nwaogu, U. C., Blawert, C., Scharnagl, N., Dietzel, W., & Kainer, K. U. (2009). Influence of inorganic acid pickling on the corrosion resistance of magnesium alloy AZ31 sheet. Corrosion Science, 51(11), 2544-2556.

60. Ghali, E., Dietzel, W., & Kainer, K. U. (2004). General and localized corrosion of magnesium alloys: a critical review. Journal of materials engineering and performance, 13(1), 7-23.

61. Mutombo, K., & Du Toit, M. (2011). Corrosion fatigue behaviour of aluminium alloy 6061-T651 welded using fully automatic gas metal arc welding and ER5183 filler alloy. International Journal of Fatigue, 33(12), 1539-1547.

62. Reichek, K. N., Clark, K. J., & Hillis, J. E. (1985). Controlling the salt water corrosion performance of magnesium AZ91 alloy. SAE transactions, 318-329.

63. Song, G. L., & Atrens, A. (1999). Corrosion mechanisms of magnesium alloys. Advanced engineering materials, 1(1), 11-33.

64. Rong-chang, Zeng, and others.”Review of studies on corrosion of magnesium alloys” Transactions of Nonferrous Metals Society of China, 763-771 (2006).

65. Gusieva, K., and others. “Corrosion of magnesium alloys: the role of alloying” International Materials Reviews, 169-194. (2015).

66. He, Y., Peng, C., Feng, Y., Wang, R., & Zhong, J. (2020). Effects of alloying elements on the microstructure and corrosion behavior of Mg–Li–Al–Y alloys. Journal of Alloys and Compounds, 834, 154344.

67. Song, Y., Han, E. H., Shan, D., Yim, C. D., & You, B. S. (2012). The role of second phases in the corrosion behavior of Mg–5Zn alloy. Corrosion Science, 60, 238-245.

68. G. Song and A. Atrens (1999) Corrosion mechanisms of magnesium alloys. Advanced Engineering Materials, 1(1), 11–33.

69. Bhargava, A. K., & Banerjee, M. K. (2017). 2.14 Heat-Treating Copper and Nickel Alloys.

70. Incesu, A., & Gungor, A. (2020). Mechanical properties and biodegradability of Mg–Zn–Ca alloys: homogenization heat treatment and hot rolling. Journal of Materials Science: Materials in Medicine, 31(12), 1-12.

71. Kuwahara, H., Al-Abdullat, Y., Ohta, M., Tsutsumi, S., Ikeuchi, K., Mazaki, N., & Aizawa, T. (2000). Surface reaction of magnesium in Hank's solutions. In Materials science forum (Vol. 350, pp. 349-358). Trans Tech Publications Ltd.

72. Thirumalaikumarasamy, D., Shanmugam, K., & Balasubramanian, V. (2014). Comparison of the corrosion behaviour of AZ31B magnesium alloy under immersion test and potentiodynamic polarization test in NaCl solution. Journal of Magnesium and Alloys, 2(1), 36-49.

73. Tonna, C., Wang, C., Mei, D., Lamaka, S. V., Zheludkevich, M. L., & Buhagiar, J. (2022). Biodegradation behaviour of Fe-based alloys in Hanks' Balanced Salt Solutions: Part I. material characterisation and corrosion testing. Bioactive materials, 7, 426-440.

74. Vidal, C. V., & Muñoz, A. I. (2008). Electrochemical characterisation of biomedical alloys for surgical implants in simulated body fluids. Corrosion Science, 50(7), 1954-1961.

75. Esmailzadeh, S., Aliofkhazraei, M., & Sarlak, H. (2018). Interpretation of cyclic potentiodynamic polarization test results for study of corrosion behavior of metals: a review. Protection of metals and physical chemistry of surfaces, 54(5), 976-989.

76. Di Gianfrancesco, A. (2017). Technologies for chemical analyses, microstructural and inspection investigations. In Materials for ultra-supercritical and advanced ultra-supercritical power plants (pp. 197-245). Woodhead Publishing.

77. Oud, J. H., & Jansen, R. A. (2000). Continuous time state space modeling of panel data by means of SEM. Psychometrika, 65(2), 199-215.

78. Liu, L., Yuan, F., Zhao, M., Gao, C., Feng, P., Yang, Y., ... & Shuai, C. (2017). Rare earth element yttrium modified Mg-Al-Zn alloy: Microstructure, degradation properties and hardness. Materials, 10(5), 477.

79. Li, M., Li, C., Liu, X., & Xu, B. (2009). Effect of Nd on microstructure and mechanical properties of AZ31 magnesium alloy. Rare metal materials and engineering, 38(1), 7-10.

80. Wang, Z., Ye, F., Chen, L., Lv, W., Zhang, Z., Zang, Q., ... & Lu, S. (2021). Preparation and Degradation Characteristics of MAO/APS Composite Bio-Coating in Simulated Body Fluid. Coatings, 11(6), 667.

81. Ralston, K. D., Fabijanic, D., & Birbilis, N. (2011). Effect of grain size on corrosion of high purity aluminium. Electrochimica acta, 56(4), 1729-1736.

82. Zhou, W., Shen, T., & Aung, N. N. (2010). Effect of heat treatment on corrosion behaviour of magnesium alloy AZ91D in simulated body fluid. Corrosion Science, 52(3), 1035-1041.

83. Peng, L. M., Chang, J. W., Guo, X. W., Atrens, A., Ding, W. J., & Peng, Y. H. (2009). Influence of heat treatment and microstructure on the corrosion of magnesium alloy Mg-10Gd-3Y-0.4 Zr. Journal of Applied Electrochemistry, 39(6), 913-920.

84. Bakhsheshi-Rad, H. R., Abdul-Kadir, M. R., Idris, M. H., & Farahany, S. J. C. S. (2012). Relationship between the corrosion behavior and the thermal characteristics and microstructure of Mg–0.5 Ca–xZn alloys. Corrosion Science, 64, 184-197.

85. Song, G. L., & Atrens, A. (1999). Corrosion mechanisms of magnesium alloys. Advanced engineering materials, 1(1), 11-33.

86. Zhao, M. C., Liu, M., Song, G., & Atrens, A. (2008). Influence of the β-phase morphology on the corrosion of the Mg alloy AZ91. Corrosion Science, 50(7), 1939-1953.

87. Song, G., & Xu, Z., "The surface, microstructure and corrosion of magnesium alloy AZ31 sheet", Electrochemical Acta, 55(13): 4148-4161 (2010).

88. Lu, Y., Bradshaw, A., Chiu, Y., & Jones, I., "Effects of secondary phase and grain size on the corrosion of biodegradable Mg–Zn–Ca alloys", Materials Science and Engineering: C, 48: 480-486 (2015).

89. Metalnikov, P., Hamu, G., Templeman, Y., Shin, K., & Meshi, L., "The relation between Mn additions, microstructure and corrosion behavior of new wrought Mg-5Al alloys", Materials Characterization, 145: 101-115 (2018).

90. Feng, H., Liu, S., Du, Y., Lei, T., Zeng, R., & Yuan, T., "Effect of the second phases on corrosion behavior of the Mg-Al-Zn alloys", Journal of Alloys and Compounds, 69, s. 2330-2338 (2017). 211

91. Aung, N., & Zhou, W., "Effect of grain size and twins on corrosion behavior of AZ31B magnesium alloy", Corrosion Science, 52(2): 589-594 (2010).

92. D. Wan, Y. Hu, S. Ye, Z. Li, L. Li, and Y. Huang, Effect of Alloying Elements on Magnesium Alloy Damping Capacities at Room Temperature, Int. J. Miner. Metall. Mater., 2019, 26(6), p 760–765.

93. StJohn, D. H., Easton, M. A., Qian, M., & Taylor, J. A. (2013). Grain refinement of magnesium alloys: a review of recent research, theoretical developments, and their application. Metallurgical and materials transactions A, 44(7), 2935-2949.

94. Koç, E., Incesu, A., & Saud, A. N. (2022). Comparative Study on Dry and Bio-Corrosive Wear Behavior of Mg-xAl-3Zn Alloys (x= 0.5-1-2-3 wt.%). Journal of Materials Engineering and Performance, 31(1), 613-621.

95. Mena-Morcillo, E., Veleva, L., & Wipf, D. O. (2018). In situ investigation of the initial stages of AZ91D magnesium alloy biodegradation in simulated body fluid. Int. J. Electrochem. Sci, 13, 5141-5150.

96. Mena-Morcillo, E., & Veleva, L. (2020). Degradation of AZ31 and AZ91 magnesium alloys in different physiological media: Effect of surface layer stability on electrochemical behaviour. Journal of Magnesium and Alloys, 8(3), 667-675.

97. Raghavan, V. (2007). Al-Gd-Mg (Aluminum-Gadolinium-Magnesium). Journal of Phase Equilibria and Diffusion, 28(5), 464-468.

98. Wu, G., Wang, C., Sun, M., & Ding, W. (2021). Recent developments and applications on high-performance cast magnesium rare-earth alloys. Journal of Magnesium and Alloys, 9(1), 1-20.

RESUME

Ahmed Saad Najm AL-JUBOURI was born in 1996 in Baghdad, after completing his primary and secondary education in Baghdad, he started a bachelor's program at the University of Technology in Iraq, Department of Production and Metallurgy Engineering, specializing in CAD/CAM in 2014 and graduated in 2018. He was accepted into Karabuk University in the Department of Materials and Metallurgy Engineering, starting a master's program in 2020 and graduating in 2022.